EXPERIMENTAL SIMULATION OF ARSENIC TRIOXIDE LEACHING AND MECHANISM OF ARSENITE OXIDATION IN SOIL

by

ZIMING YUE

RONA J. DONAHOE, COMMITTEE CHAIR

FRED ANDRUS
PERRY CHURCHILL
JENNIFER W. EDMONDS
GEOFFREY R. TICK
DIMITRI VLASSOPOULOS

A DISSERTATION

Submitted in partial fulfillment of the requirements
for the degree of Doctor of Philosophy
in the Department of Geological Sciences
in the Graduate School of
The University of Alabama

TUSCALOOSA, ALABAMA

2012

ABSTRACT

Arsenic trioxide was widely applied to soils in North America as an herbicide during the 1950-60s. These herbicide applications led to soil arsenic contamination at numerous sites. Decades after the herbicide application, the contaminated soil served as a secondary source for long-term leaching of arsenic into the groundwater system. To understand the history of arsenic contamination at these sites, column experiments were conducted to simulate the herbicide application and subsequent arsenic leaching processes. The experimental data showed that the effluent solution arsenic became dominantly As(V) after 180 pore volumes (equivalent to ~60 years of natural leaching, assuming a 50% recharge rate) of leaching, which represented an abnormally rapid arsenite oxidation rate (up to 60 mg/L/6.5 hours As(V)) (Yue and Donahoe, 2009). During peak arsenic release, the arsenite oxidation rate doubled (120 mg/mL/6.5 hours). Homogeneous As(III) oxidation cannot be responsible for the observed oxidation rate because the half life of As(III) in air can be up to one year (Eary and Schramke, 1990). Incubation experiments were designed, where sterilized and inoculated serum bottles with added aqueous As(III) and soil were compared for their aqueous total arsenic and As(V) concentrations. The aqueous As(V) in the innoculated series increased with time but remained below detection in the sterile series. This indicated that the As(III) oxidation observed in the column experiments was caused by the microbes in the soil.

Bacterium strains A4 and A12 were isolated from the column soil and were tested to be the efficient arsenite oxidizers in the column experiments. Strain A12 shared 100% 16S rDNA sequence with *B. fungorum* LMG 16225^{T}, while strain A4 shared 99.1%, 97.3% and 96.7% 16S

rDNA sequences with strains *B. zhejiangensis* CCTCC AB 2010354^T, *B. glathei* DSM 50014^T and *B. sordidicola* KCTC 12081^T, respectively.

A polyphasic characterization, including phenotypic and biochemical characterization, 16S rDNA sequence analysis, DNA-DNA hybridization, and fatty acid analysis, was conducted on strain A4 to determine its taxonomic position. The results showed that strain A4 represented a novel species in the genus *Burkhoderia*, for which the name *Burkholderia arsenicoxydans* sp. nov. is proposed. The type strain is A4^T (=ATCC BAA-2404^T=CCTCC AB 2012027^T).

DEDICATION

To my family, Lihua, Shuwen, and April.

LIST OF ABBREVIATIONS AND SYMBOLS

As	Arsenic
ATCC	American type culture collection
CCTCC	China center for type culture collection
CCUG	Culture Collection, University of Göteborg, Sweden
DDI	Doubly deionized (water)
DNA	Deoxyribonulceic acid
DSMZ	Deutsche Sammlung von Mikroorganismen und Zellkulturen GmbH (German Collection of Microorganisms and Cell Culture)
EPA	Environmental protection agency
ESI MS	Electrospray ionization mass spectrometer
FW	The column that contained 10” Blank FW soil
FWAs	The column that contained 10” FW soil+(1/6)”arsenic trioxide
FWAsG	The column that contained 10” FW soil+(1/6)”arsenic trioxide +(1/2)” carbonate gravel
FW2AsG	The column that contained 10” FW soil+(1/3)”arsenic trioxide +(1/2)” carbonate gravel
GC	Gas chromatograph
GTR	General Time Reversible (GTR) model
HPLC	High pressure liquid chromatography
IC	Ion chromatograph

ICP-MS	Inductively coupled plasma-mass spectrometer
ICP-OES	Inductively coupled plasma optical emission spectrophotometer
KCTC	Korean collection for type cultures
LMG	Laboratorium voor Microbiologie Universiteit Gent=BCCM= Belgian Co-ordinated Collections of Micro-organisms
MIDI	MIDI company
MWD	Microwave-assisted acid digestion
PCR	Polymerase chain reaction
PE	Phosphatidylethanolamine
PG	Phosphatidylglycerol
Rf	Retention factor for thin layer chromatography
SEM	Scanning electron microscope
SPLP	Synthetic precipitation leaching procedure
TCE	Trichloroethylene
TEM	Transmission electron microscope
TLC	Thin layer chromatography
XANES	X-ray absorption near edge structure
XRD	X-ray diffraction

ACKNOWLEDGMENTS

I would like to thank my PhD supervisor, Dr. Rona J. Donahoe, for her many years of academic guidance and research support as a genuine and devoted scientist. As an academic advisor and a very good personal friend with a warm and patient heart, she has helped me develop in both my graduate career and my family development.

I also would like to thank other committee members Dr. Fred Andrus, Dr. Perry Churchill, Dr. Jennifer Edmonds, Dr. Geoffrey Tick, Dr. Dimitri Vlassopoulos for their guidance and patient support through my PhD path.

I very much appreciate Dean Francko's support, Department of Geological Sciences support, Dr. Zheng's research fund, GSAB scholarships, Graduate School research fund, GCAGS research fund, and Graduate Student Association research fund.

Special thanks to Betsy Graham for her help in the Analytical Geochemical Lab and Alex Teoh for his help in the Molecular Systematic Facility Lab. Two of the contributions of this dissertation were directly associated with their help, respectively. Certainly, thanks to people who created the research environments and/or guided me there.

I would like to thank my labmates Yongqiang Qi, Sid, Hari, and Ningning Sun. In addition, Li Yang, who, although we never met, provided much help. I also want to thank Betty, Debbie, and Darlene in the Department of Geological Sciences office for their kindness and warm-heartedness. They are always there to provide a selfless hand.

I would like to thank the many labs in the Department of Chemistry and the Department of Biological Sciences. The faculty, staff and students in those departments gave me time, space, and technical support. I am grateful for the Southern Company Services project that started this research, and also thank the Groundwater Division at the Geological Survey of Alabama for supporting me to complete the research.

I would also like to thank First Baptist Church for their help in spiritual and everyday life. They provided immediate help when I needed it. Many thanks to my Chinese and international friends and American host families, they made my family's life in United States and the University of Alabama easier and happier.

Finally, I thank my family, my parents, especially my wife, Lihua Guo, and beautiful daughters Shuwen and April, their love, hard work, dedication, and constant support that encouraged me to make my dream come true.

CONTENTS

LIST OF TABLES

Chapter 4.

LIST OF FIGURES

Chapter 2.

Chapter 3.

CHAPTER 1

INTRODUCTION

People generally know arsenic as a poison; however, it is less well-known that arsenic is a ubiquitous element that is found in the atmosphere, soils, and rocks. In the natural environment, high arsenic concentrations in soils are usually associated with sulfide deposits and their weathering products. Human activities, such as sulfide mining, smelting, combustion of fossil fuels, and application of arsenical herbicides, can also lead to high arsenic concentrations in soil and groundwater.

Arsenic is of concern mostly because of the toxic properties of a number of its inorganic species in the environment. Arsenic toxicity depends on its concentration and its mobility, which depends on speciation. Although arsenic can exist in four oxidation states (-3, 0, +3, and +5) in the natural environment, arsenate (As(V)) and arsenite (As(III)) are the major soil species. Arsenite is 50 times more toxic than arsenate. Arsenite is more mobile and bioavailable than arsenate due to its tendency to form outer-sphere complexes on mineral surfaces, which are less strongly held and therefore more mobile and bioavailable in the environment. Arsenite strongly bonds with cysteine in proteins, which impairs protein function. Arsenate toxicity is due to its ability to inhibit adenosine triphosphate (ATP) synthesis, where ATP is a fundamental energy source for life. Arsenate enters cells through phosphate transporters due to their molecular similarity, while arsenite enters cells through aqua-glyceroporins (Oremland & Stolz, 2003).

The Fort Walton (FW) site arsenic contamination was caused by arsenic trioxide herbicide application in the 1950s. Solid arsenic speciation and arsenic leachability studies showed the arsenic in the soil exists as As(V) and only a small amount of arsenic is leachable, which could make *in-situ* fixation remediation possible (Yang & Donahoe, 2007). However, the arsenic contamination process and the fate of the leached arsenic were not known. The purpose of this dissertation is to use soil column experiments to simulate the arsenic contamination process and to determine the controlling factors in the process, providing further insight into the fate and potential remediation strategies for the arsenic-contaminated field site.

This dissertation consists of three stand-alone papers:

Chapter two discusses the experimental simulation of soil contamination by arsenic trioxide. The experimental setup was scaled down from the FW site by a ratio of 6:1, including the background soil lying above the water table, the variable thickness of arsenic trioxide, and the existence of a limestone gravel cover. The chapter focuses on the transformation of arsenic oxidation state with leaching time, without consideration of the oxidation mechanism. The goals of this work are to provide more insight into the herbicide contamination process, to enable better prediction of the long-term fate of soil arsenic and the leaching of arsenic into groundwater.

Chapter three investigates the mechanism of arsenite oxidation in the soil column experiments. Sixty years after the application of herbicide, the arsenic in the contaminated soil at the FW site is entirely As(V). Experimental simulation of the arsenic trioxide contamination process also led to the production of 60 mg/L As(V) within the solution column residence time of 6.5 hours after 180 pore volumes. This abnormally rapid As(III) oxidation, if employed properly, could be used for remediation of arsenite-contaminated soil at similar sites. Hence, it is

necessary to reveal the mechanism of the As(III) oxidation. Sterile and unsterile series of serum bottle experiments, both containing aqueous As(III) and soil, were designed to compare their As(V) production with time. The results showed the As(V) in the unsterile series increased with time, while the As(V) in the sterile series kept below detection with time. This showed microbes in the soil oxidized As(III) to As(V) in the unsterile serum bottles series and in column experiments. The As(III) oxidizers were further isolated from the column soils and characterized primarily.

Chapter four discusses the characterization and nomenclature of *Burkholderia arsenicoxidans* sp. nov., an arsenite-oxidizing bacterium isolated from arsenic trioxide-contaminated soil. Two strains of As(III) oxidizing bacteria A4 and A12 were isolated from the column experiments. Strain A12 was identified as *Burkhoderia fungorum*. A4 was closest to *Burkhoderia zhejiangensis* CCTCC AB 2010354^T, *Burkhoderia glathei* DSM 50014^T with 16S rDNA similarities of 99.1% and 97.3%, respectively. A polyphasic characterization was conducted on strain A4 to determine its taxonomic position. Both strain A4 and A12 were potential to be used in arsenite soil remediation.

This entire dissertation focuses on understanding arsenic trioxide contamination of soil and groundwater, and identifying potential remediation strategies.

References

Dragun, J., Chiasson, A., 1991. Elements in North American Soils. Hazardous Materials Control Resources Institute, Greenbelt, MD.

Huang, Y.-C. 1994. Arsenic distribution in soils. pp. 17-49. In: Nriagu, J. O. (Ed.), Arsenic in the environment Part I: Cycling and characterization. John Wiley & Sons, Inc., New York,

National research council, 1977. Arsenic. National academy of sciences, Washington D. C.

Oremland, R. S., Stolz, F. S. 2003. The ecology of arsenic. Science. 300: 939-944

Yang, L., Donahoe, R. J., 2007. The form, distribution and mobility of arsenic in soils contaminated by arsenic trioxide, at sites in southeast USA. Applied Geochemistry. 22: 320-341

CHAPTER 2

EXPERIMENTAL SIMULATION OF SOIL CONTAMINATION BY ARSENIC TRIOXIDE

Abstract

Column experiments were conducted to experimentally simulate the initial conditions at a field site where legacy arsenic contamination was caused by application of arsenic trioxide as an herbicide to the soil. The experiments were designed to investigate the influence of herbicide loading and carbonate gravel on the release of arsenic to, and the arsenic adsorption capacity of, the background soil. The results showed that the arsenic released from the doubly spiked column was three times higher than for the singly spiked columns. The addition of gravel above the herbicide layer halved the leaching time needed for peak arsenic release from the soil. The columns with carbonate gravel retained more arsenic (15.6 g for column FWAsG and 12.3 g for column F2AsG) than the column without arsenic trioxide (0.13 g for column FWAs). The results also indicated the thickness of the arsenic trioxide layer was not important in terms of the arsenic retention capacity of the soil columns. Arsenate was detected and quantified in the effluent solutions by ion chromatography (new contribution). The data indicated As(III) dominated in the effluents for the first 180 pore volumes (PVs). After 180 PVs, As(III) almost disappeared and As(V) dominated in the effluents. This abrupt drop in As(III) concentrations and the unexpected high arsenic peak release from the doubly spiked column FW2AsG were interpreted as higher As(III) concentration had higher capability to dissolve arsenic trioxide by solute-solute

interaction or polymerization. Effluent solution Eh-pH values indicated that As(V) was the thermodynamically stable form of arsenic throughout the experiments. Therefore, As(III) dominance in the initial column effluent solutions was kinetically controlled.

Keywords: Arsenic, arsenic trioxide, herbicide, contamination, experimental

1. Introduction

Arsenic is a ubiquitous element found in the atmosphere as well as in soils and rocks. Its crustal abundance is 1.5 to 2 ppm (National Research Council, 1975), while the average arsenic concentration in soils is around 5 ppm (Dragun & Chiasson, 1991; Huang, 1994). High arsenic concentrations in natural soils are usually associated with sulfide deposits and their weathering products. Human activities, such as sulfide mining, smelting, combustion of fossil fuels, and use of arsenical herbicides and other chemicals can often lead to elevated arsenic concentrations in soil and groundwater. Arsenic is of concern because of the toxic properties of a number of its inorganic species in the environment. Organic arsenic species, though toxic, are usually quantitatively insignificant. Arsenic toxicity depends on its concentration and speciation. Arsenic speciation and mobility depend on pH and Eh. It is unique among the heavy metalloids and oxyanion-forming elements in that it becomes more mobile at reduced conditions and differs from heavy metals in becoming more mobile as pH increases (Smedley & Kinniburgh, 2002). In the natural environment, arsenic may exist in four oxidation states: -3, 0, +3, and +5. Arsenate (As(V)) and arsenite (As(III)) are the primary forms of arsenic in soils.

Arsenic trioxide (arsenic trioxide) was used as an herbicide at many industrial sites prior to 1970 (Huang, 1994). Especially in North America, arsenic trioxide applications have

contaminated soils with hundreds of ppm arsenic at thousands of sites. The purpose of this study was to experimentally simulate a 50 year old field site where arsenic trioxide was applied to soil as an herbicide and resulted in legacy arsenic contamination of soil and groundwater. To obtain source term parameters needed to model arsenic release from these sites and subsequent transport of arsenic in the subsurface, column experiments were conducted to simulate site conditions following arsenic herbicide application. The experiments were designed to provide the following information: 1) the rate of arsenic release under natural leaching conditions; 2) the arsenic adsorption capacity and leaching behavior of the background soil; 3) the effect of a limestone gravel layer on arsenic mobility; and 4) scaling of herbicide layer thickness.

2. Materials and methods

2.1. Arsenic trioxide (As_2O_3)

The arsenic trioxide (99% purity) used in the experiments was purchased from Pfaltz & Bauer. Arsenic trioxide has a molecular lattice with a cage molecule of As_4O_6. The As-O-As bond in the molecule is unstable upon hydrolysis. The arsenic forms $As(OH)_3$ upon dissolution.

2.2. Background soil

Uncontaminated (background) surface soil samples were collected from the same soil unit near a contaminated site located in Florida. The soil samples were passed through a 1 mm screen to remove debris, air dried and thoroughly homogenized by mixing. The soil is a yellow sandy loam in which quartz sand accounts for more than 99% of the soil, by weight. To characterize the clay-sized fraction of the soil, a standard settling/filtration technique was used to

remove most of the quartz and concentrate the clay minerals in an oriented mount for X-ray diffraction (XRD) analysis. A Bruker D8 Advance powder XRD system was used to obtain the diffraction pattern.

Figure 2-1 shows the XRD pattern of the background soil's clay fraction. The mineral composition of the soil is predominantly quartz, with chlorite, muscovite and minor kaolinite. The environmentally available arsenic concentration of the background soil was 1.88 ppm, as determined by microwave-assisted acid digestion (MWD) of the dry, homogenized soil using US EPA Method 3051A (1994a). The soil pH was measured as 7.11, according to US EPA Method 9045C (1995).

2.3. Column setup

The dried, homogenized soil was packed into four 4×18 inch Plexiglas columns (Figure 2-2) having an inner diameter of 3.46 inches. The columns were designed at a 1:6 scale compared to the field site and constructed to separate the influence of the different site parameters: Column FW consisted of 10 inches of background soil; Column FWAs consisted of 1/6 inch of As_2O_3 on 10 inches of background soil; Column FWAsG consisted of 1/6 inch of As_2O_3, plus 1/2 inch limestone gravel on 10 inches of background soil; Column FW2AsG consisted of 1/3 inch of As_2O_3, plus 1/2 inch limestone gravel on 10 inches of background soil.

Before leaching was initiated, 18.0 MΩ doubly deionized (DDI) water was pumped into the bottom of the columns to saturate the soil. The water volumes required to saturate the packed materials were recorded as the pore volumes of the columns (582.5 cm^3 for FW; 571.25 cm^3 for FWAs, 586.25 cm^3 for FWAsG, and 643.75 cm^3 for FW2AsG). The initial column pore volume was used as the x-axis unit for column effluent composition plots (see figure 2-3). Next,

synthetic precipitation leaching procedure solution (SPLP; pH 4.2) was made according to US EPA Method 1312B (1994b) and continuously pumped into the top of the columns at 1.2 ml/min to begin the leaching experiments.

2.4. Chemical analyses

Periodically, effluent samples (40 ml each) were taken simultaneously from each column, the pH and Eh were measured and the samples were filtered through 0.2 μm nylon syringe filters. The samples for cation analyses were acidified to 2% HNO_3 by volume, using Optima™ ultrapure nitric acid and analyzed using a Perkin Elmer Optima 3000 DV inductively coupled plasma optical emission spectrophotometer (ICP-OES). The FW column effluent samples and background soil MWD supernatants were analyzed for arsenic using a Perkin Elmer Sciex Elan 6000 inductively coupled plasma-mass spectrometer (ICP-MS), due to their low arsenic concentrations. Anion samples were kept frozen until analysis by ion chromatography. Anion (sulfate, nitrate, fluoride, chloride, bromide, oxalate and arsenate) concentrations were measured using a Dionex 600 Ion Chromatograph (IC).

3. Results

The column effluent samples were analyzed for 22 cations and for 6 anions, including arsenate. Only a portion of the chemical data is presented here due to space limitations.

3.1. Total arsenic release

Effluent arsenic concentrations peaked at 1000 to 3000 ppm for the spiked soil columns. The graveled columns (FWAsG and FW2AsG) reached their arsenic peaks (1138.5 and 3099.2

ppm, respectively) after approximately 30 pore volumes (PVs) of fluid flow, earlier than the arsenic peak of 1253.8 ppm at 51.4 PVs for column FWAs (Figure 2-3). This indicates that the presence of carbonate gravel increases the rate of arsenic release from the herbicide and/or lowers retention of the arsenic by the soil. In contrast to the As-spiked columns, the background soil column (FW) showed steady arsenic release of around 0.0018 ppm.

3.2. Effluent solution pH

The effluent solution pH of the background soil column (FW) decreased gradually from around 7.3 to about 4.5 over the leaching period. In contrast, the pH of the three spiked column effluents decreased rapidly from around 7 to just above 3, then increased gradually to approach the SPLP solution pH of 4.2. Minimum pH was reached by column FWAsG around 100 PVs, and at around 150 PVs for FWAs and FW2AsG. During the subsequent pH increase, column FWAs effluent maintained slightly lower pH than that of columns FWAsG and FW2AsG (Figure 2-4).

3.3. Arsenate concentrations

Figure 2-5 shows effluent arsenate concentration trends from the three arsenic-spiked columns. Arsenate concentrations gradually increased through about 30 PVs, then showed rapid increases to peak at 175-273 ppm between 100-170 PVs of fluid flow. Compared to the total arsenic leaching trends, the arsenate peaks were significantly lower in concentration and much broader, especially for column FWAsG effluents. After about 170 PVs of fluid flow, the arsenate concentrations of the spiked column effluents steadily decreased. Column FWAs showed higher arsenate concentrations than FWAsG and FW2AsG after 200 PVs of fluid flow. The overall

arsenate concentration trends were generally opposite to those for pH, with highest effluent arsenate concentrations correlating with minimum pH.

4. Discussion

4.1. Comparison between total arsenic and As(V)

The effluent solution arsenate concentration data from ion chromatography were converted to As(V) and plotted with the total arsenic data from ICP-OES. Figure 2-6 and Figure 2-7 show the data for column experiments FWAs and FWAsG. The results show that the total arsenic concentration was more than an order of magnitude higher than that of As(V) at peak arsenic release, indicating that almost all of the arsenic was initially released from the herbicide as As(III). After approximately 200 PVs, however, all of the eluted arsenic was in the +5 valence state. A similar comparison between total arsenic and As(V) was observed for column FW2AsG. Figure 2-8 shows the distribution of arsenic species as a function of Eh and pH, and was constructed using new thermodynamic data given by Nordstrom and Archer (2003). As shown in Figure 2-6, the measured Eh-pH values of the column effluent samples plot in the stability fields of aqueous As(V) species, predominantly within the $H_2AsO_4^-$ stability field. Although As(V) is the thermodynamically favored form of arsenic, the previous discussion demonstrates that it does not predominate in the effluent solutions until most of the arsenic has eluted as As(III). These results indicate that the initial column effluent solutions had not achieved chemical equilibrium and that the persistence of $H_3AsO_3^\circ$ in the initial effluent solutions was due to the slow oxidation rate of As(III) to As(V). Over longer time scales, As(III) is expected to convert to As(V), which would reduce arsenic mobility. In addition, the pH of the spiked column effluents slowly

increases after 200 PV due to mineral buffering reactions predominating over hydrolysis of As(III) to As(V).

4.2. Arsenic trioxide dissolution/hydrolysis

The arsenic trioxide structure is based on a cage molecule (As_4O_6). Upon dissolution, the As-O-As bond breaks to form the $As(OH)_3$ aqueous species which has a pyramidal structure.

$$As_2O_{3(cubic)} + 3H_2O_{(l)} = 2As(OH)_{3(aq)} \quad (1)$$

For the above reaction, $\Delta_r G° = 7.667$ kJ/mol, so arsenic trioxide hydrolysis is not spontaneous at standard state (i.e., pure water and 1 m $As(OH)_{3(aq)}$). However, low dissolved arsenic concentrations will favor the forward reaction. Reaction (1) reaches equilibrium only at high $As(OH)_{3(aq)}$ activity, i.e., $10^{-0.8}$ m (Vink, 1996). $As(OH)_{3(aq)}$ activities in the current column experiments were significantly lower than $10^{-0.8}$ m, hence the arsenic trioxide tended to dissolve. But the kinetics of arsenic trioxide hydrolysis is slow; it may take several weeks for the dissolution reaction to reach equilibrium (National Research Council, 1977). In fact, the rate of arsenic trioxide dissolution observed in this study was much slower than previously reported. Figure 2-9 shows that 0.02 g of arsenic trioxide did not dissolve completely in one liter of water at room temperature over a 14 month period. Subsequent heating increased the rate of dissolution (Figure 2-9), but even after heating, only 80% of the arsenic trioxide dissolved.

The published arsenic trioxide solubility of 2.05 g arsenic trioxide per 100 g water at 25˚C was measured by dissolving excess arsenic trioxide powder in hot water (100˚C), then cooling to the required temperature to achieve equilibrium (Story et al., 1923). We were unable to duplicate this extremely high solubility value using the reported procedure.

4.3. Observation of arsenic trioxide residue

Figure 2-10 shows an SEM image of residual arsenic trioxide from the top of column FWAs. At a scale of 1 μm, all angular parts of the residue were observed to be rounded. In addition, no fine grains of arsenic trioxide remained on the surfaces of the larger crystals. Arsenic trioxide has a molecular lattice and hence even lower surface energy than covalently bonded crystals such as quartz. Preferential dissolution of the micro-angular and fine-grained fractions of the arsenic trioxide is driven by the higher surface energy of these materials. The arsenic release peaks at the beginning of the experiments are likely related to the rapid dissolution of the fine-grained and microangular fractions of the arsenic trioxide powder.

4.4. Effect of the carbonate gravel layer

The previous discussion showed that arsenic trioxide hydrolysis is non-spontaneous at standard state. Although the $As(OH)_2CO_3^-$ complex can increase arsenic trioxide solubility, Neuberger and Helz (2004) determined that it was not significant in natural systems. Arsenic trioxide hydrolysis therefore likely occurs in alkaline solutions via the following two reactions:

$$As_2O_{3(cubic)} + H_2O_{(l)} + 2OH^- = 2H_2AsO_3^- \qquad \Delta_rG° = -47.173 \text{ kJ/mol} \qquad (2)$$

$$H_2AsO_{3\,(aq)}^- + H^+ = As(OH)_{3(aq)} \qquad \Delta_rG° = -52.37 \text{ kJ/mol} \qquad (3)$$

The free energy changes of these reactions indicate that arsenic trioxide hydrolysis in alkaline solutions is spontaneous, even at standard state. The SPLP solution (pH 4.2) reacted with the carbonate gravels and the leachate pH was increased by calcium carbonate dissolution. This reaction pathway explains why the spiked columns with carbonate gravel had earlier arsenic release peaks at the beginning of the experiments than the spiked column without carbonate gravel.

4.5. As(III) oxidation to As(V)

From the effluent pH vs PV plot (Figure 2-4), it is apparent that all of the spiked columns had rapid pH drops at the beginning of the experiments. The decrease in leachate pH was caused by As(III) oxidation to As(V). The As(V) and total As comparison curves (Figures 2-6 and 2-7) show that after approximately 200 PVs, all arsenic in the spiked column effluents was As(V). Despite this observation, abundant arsenic trioxide (As(III)) still remained at the tops of the spiked columns after 200 PV of fluid flow.

Addressing the question of whether the As(III) was oxidized to As(V) at the arsenic trioxide surface or within the soil columns, consider the following reactions:

$$As_2O_{3(cubic)} + O_{2(g,\ 0.2\ atm)} = As_2O_{5(cr)} \qquad \Delta_rG° = -194.63\ kJ/mol \qquad (4)$$

$$As_2O_{5(cr)} + 3H_2O_{(l)} = 2H_2AsO_4^- + 2H^+ \qquad \Delta_rG° = -20.806\ kJ/mol \qquad (5)$$

Arsenic trioxide at the tops of the spiked columns was exposed to atmospheric oxygen, and its oxidation via reaction (4) has a strong thermodynamic drive. This reaction is limited to the arsenic trioxide surface. The oxidation product, $As_2O_{5(cr)}$, is hygroscopic and its hydrolysis via reaction (5) is spontaneous. Hence, reaction pathway (4) + (5) is a possible oxidation mechanism.

In addition, the aqueous species $As(OH)_3$ can also be oxidized in solution:

$$2As(OH)_{3(aq)} + O_{2(aq)} = 2H_2AsO_4^- + 2H^+ \qquad \Delta_rG° = -243.64\ kJ/mol \qquad (6)$$

This reaction has an even stronger thermodynamic drive $\Delta_rG° = -243.64$ kJ/mol, but is limited by the availability of aqueous oxygen. Although there is no additional oxygen supply to the soil columns, the initial SPLP solution was approximately saturated with respect to atmospheric oxygen and reaction pathway (6) is therefore also possible.

To test the relative importance of these oxidation reaction pathways, SPLP leachate solution was allowed to stand for 7 hours at the tops of the spiked columns in contact with the

arsenic trioxide, then sampled and analyzed within 24 hours for total arsenic and As(V). The results showed that 25%, 90% and 96% of the total arsenic in the aqueous samples was As(V) for columns FWAs, FWAsG and FW2AsG, respectively. The As(V) percentage was significantly lower for column FWAs than the value of 100% measured in the effluent solutions. These results show that reaction pathway (6) was significant for the column without the gravel layer, with 75% of the total arsenic being oxidized within the soil columns, probably through catalysis on soil particle surfaces. The results also indicate that reaction pathway (2) + (3) was the predominant oxidation mechanism when carbonate gravel was present, due to more extensive hydrolysis of the arsenic trioxide, as discussed above.

4.6. Arsenic retention capacity of the spiked soil columns

A total of 72.91 g As was added as a spike to columns FWAs and FWAsG, and a total of 145.82 g As was added to column FW2AsG in the form of As_2O_3 (arsenic trioxide). The area under each effluent arsenic concentration vs PV curve was integrated to determine the total arsenic leached from the spiked columns. The cumulative arsenic eluted from each spiked column is shown in Figure 2-11. Extrapolation of these curves to the point where the effluent arsenic concentrations reach the ICP detection limit of 0.02 ppm As (corresponding to 2900 PV) was used to estimate the total solubilized arsenic mass for each column (FWAs: 72.8 g; FWAsG: 57.3 g; FW2AsG: 133.52 g). The arsenic retention capacity of the soils was then calculated by mass balance: FWAs: 0.13 g; FWAsG: 15.60 g; FW2AsG: 12.30 g. For columns FWAs, FWAsG and FW2AsG, the percentage of the As spike leached was 99.8%, 78.6% and 91.6%, respectively.

From these results, it is apparent that the soil columns with an overlying carbonate gravel layer have higher arsenic retention capacities (FWAs: 48.6 mg As/kg soil; FWAsG: 5838 mg As/kg soil; FW2AsG: 4599 mg As/kg soil), sequestering between 8.4% to 21.4% of the original arsenic spike, compared to only 0.2% As sequestration without gravel. It is postulated that the gravel provided higher pH conditions and a source of calcium, enabling the formation of calcium arsenate phases within the soil. This is supported by the findings of Yang and Donahoe (2007), who used electron microprobe, XANES and μ-XRD analyses to show the presence of authigenic calcium arsenate phases in a similar soil contaminated 50 years ago by arsenic trioxide herbicide application. Of the two soils studied by Yang and Donahoe (2007), BH and FW, it was the soil with higher calcium content (BH) that had the highest arsenic concentration.

The arsenic trioxide layer thickness had a smaller impact on soil arsenic retention than the presence or absence of the gravel layer. The doubly spiked and graveled soil column (FW2AsG) retained less of the total arsenic than the graveled soil column with the single arsenic trioxide spike (FWAsG): 8.4% vs 21.4%, respectively. The total arsenic release curves (Figure 2-11) show that the greater arsenic release for FW2AsG was achieved early in the experiments. For example, at 190 pore volumes, 119 g As was released in the effluent solutions from column FW2AsG while 45 g As was released in the effluents for column FWAsG. By then, column FW2AsG had lost 74 g more As than column FWAsG. This cannot be simply explained by the double thickness of the arsenic trioxide layer for FW2AsG, as the arsenic release was more than twice that from FWAsG. Nor can the disproportionately high arsenic release be explained by the carbonate gravel because both columns had the same gravel layer thickness (and similar effluent pH and Ca concentrations). Figures 2-6 and 2-7 show that the early arsenic releases were all dominated by As(III), so the higher arsenic release from FW2AsG cannot be explained by

differences in sorption behavior of As(III) vs. As(V). The most reasonable explanation is therefore based on soil sorption kinetics which limited the rate of arsenic uptake by the soil when very high arsenic concentrations were eluting through the soil column.

4.7. Application of experimental results to field sites

The column experiments have thus far modeled more than 40 years of arsenic leaching in the field, using the average field site rainfall rate of 0.0047 ft/day and 23% precipitation infiltration, which produced a temporal scaling factor of 38.68 times. The current arsenic leaching concentrations fall within the range of current arsenic concentrations observed in groundwater monitoring wells at the field site. Despite these successes, the herbicide layer at the field site has been removed completely by natural leaching, while the spiked columns still have some arsenic trioxide residue at their tops. This may be due, in part, to the fact that the SPLP solution used as the leachate in the column experiments had an Eh around 450 mV, while Eh of natural precipitation is higher, around 581 mV (Deutch et al. 1997). This difference may have led to a slower As(III) oxidation rate, both on the arsenic trioxide surfaces and in the soil columns, compared to the natural environment.

5. Summary and conclusions

The purpose of this study was to experimentally simulate a 50 year old field site where arsenic trioxide was applied to the soil as an herbicide and resulted in legacy arsenic contamination of soil and groundwater. The experimental data obtained gives insight into processes that occurred early in the history of the site, the influence of different herbicide

application rates and the effect of gravel cover on the release of arsenic from the herbicide and its transport through the soil.

The presence of carbonate gravel significantly facilitated arsenic release at the beginning of the experiments because dissolution of the calcium carbonate made the solution pH higher and increased the extent of arsenite hydrolysis. However, the columns with a carbonate gravel layer retained more arsenic (5838 mg As/kg soil for column FWAsG and 4599 mg As/kg soil for column FW2AsG) than the column without carbonate gravel (48.6 mg As/kg soil for column FWAs) throughout the experiments. The doubly spiked column (FW2AsG) released approximately 3 times more arsenic than the singly spiked column (FWAsG) during the early part of the experiments. As the result of slow sorption kinetics, the soil with the double arsenic trioxide layer thickness showed decreased arsenic retention capacity compared to the soil with the lower arsenic trioxide spike. The arsenic retained in the soil is thought to exist as calcium arsenate-like phases, supported by previous work on present-day arsenic-contaminated FW soil (Yang and Donahoe, 2007). When the column experiments are terminated, the speciation and form of arsenic in the experimentally leached soils will be examined and compared to the contaminated soils from the field site.

It was also determined that although As(V) is the thermodynamically stable form of arsenic under the Eh and pH conditions of the experiments, dissolved arsenic was dominated by As(III) in the column effluents for approximately the first 200 PVs. After 200 PVs, As(V) became the predominant form of arsenic in the effluent solutions. As(III) oxidation to As(V) occurred both at the arsenic trioxide surface and in the soil columns; oxidation at the arsenic trioxide surface was most important for the columns with carbonate gravel. The observed initial high As(III) release and “abrupt” disappearance of As(III) in the effluent solutions were

interpreted as follows. Dissolution of the fine-grained and micro-angular part of the arsenic trioxide spikes led to high leachate As(III) concentrations. When the fine-grained and micro-angular arsenic trioxide fractions were depleted, the effluent solution As(III) concentrations dropped to approximately 15 ppm, while the As(III) to As(V) oxidation rate remained constant. Hence, only As(V) was released in the effluents after 180 PVs.

The experimental results of this study are important for evaluating the potential environmental impact of arsenic release from these sites. When scaling the experiments to longer time periods, such as 50 years, As(III) will convert to As(V), reducing arsenic mobility and toxicity over the longer time scale. The experimental data obtained are being used to develop a long-term contaminant transport model for the site, providing a very well constrained range of scaled arsenic source term data that can help reactive transport modelers achieve a higher degree of accuracy and precision in their predictions.

References

Anderson, E., Story L. G., 1923. Studies on certain physical properties of arsenic trioxide in water solution. Journal American Chemical Society 45(5), 1102 - 1105.

Deutsch, F., Hoffmann, P., Ortner, H. M, 1997. Analytical characterization of manganese in rainwater and snow samples. Analytical and Bioanalytical Chemistry. 357(1), 105-111.

Dragun, J., Chiasson, A., 1991. Elements in North American Soils. Hazardous Materials Control Resources Institute, Greenbelt, MD.

Huang, Y.-C. 1994. Arsenic distribution in soils. In: Nriagu, J. O. (Ed.), Arsenic in the environment Part I: Cycling and characterization. John Wiley & Sons, Inc., New York, pp. 17-49.

National research council, 1977. Arsenic. National academy of sciences, Washington D. C.

Neuberger, C. S., Helz, G. R. 2005. Arsenic(III) carbonate complexing. Applied Geochemistry. 20(6), 1218-1225.

Nordstrom, D. K., Archer, D. G., 2003. Arsenic thermodynamic data and environmental geochemistry. In: Welch, A. H., Stollenwerk, K. G. (Eds.), Arsenic in Ground Water: Geochemistry and Occurrence. Kluwer Academic Publishers, Boston, pp. 1-25.

Smedley, P. L., Kinniburg, D. G., 2002. A review of the source, behavior and distribution of arsenic in natural waters. Applied Geochemistry. 17, 517-568.

US EPA, 1994a. Method 3051A: Microwave Assisted Acid Digestion of Sediments, Sludges, Soils, and Oils. In: US Environmental Protection Agency, Office of Solid Waste, Test Methods for Evaluating Solid Waste, Physical/Chemical methods, 3rd ed., Washington, DC: US Government Printing Office.

US EPA, 1994b. Method 1312: Synthetic Precipitation Leaching Procedure. In: US Environmental Protection Agency, Office of Solid Waste, Test Methods for Evaluating Solid Waste, Physical/Chemical methods, 3rd ed., Washington, DC: US Government Printing Office.

US EPA, 1995. Method 9045C: soil and waste pH. In: US Environmental Protection Agency, Office of Solid Waste, Test methods for evaluating solid waste, physical/chemical methods, 3rd ed. US Government Printing Office, Washington, DC.

Vink, B. W., 1996. Stability relations of antimony and arsenic compounds in the light of revised and extended Eh-pH diagrams. Chemical Geology. 130(1-2), 21-30.

Yang, L., Donahoe, R. J., 2007. The form, distribution and mobility of arsenic in soils contaminated by arsenic trioxide, at sites in southeast USA. Applied Geochemistry. 22, 320-341.

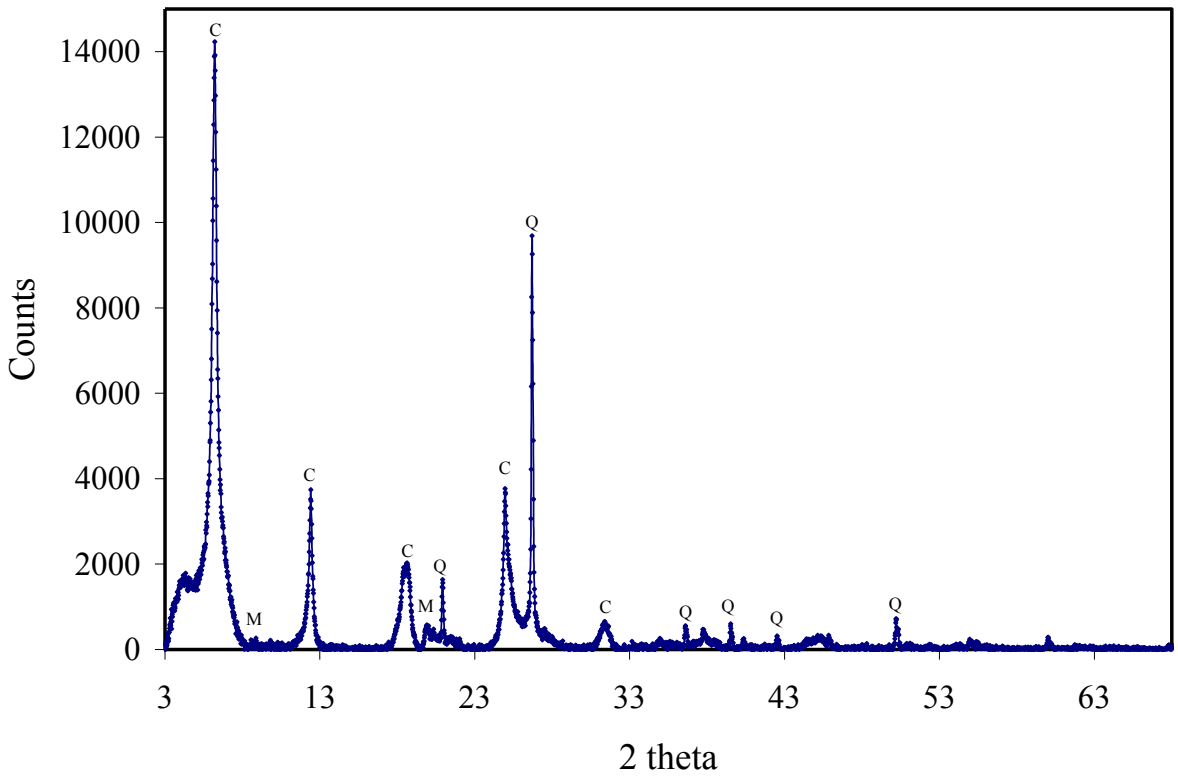

Figure 2-1. Clay smear XRD pattern of FW background soil. The soil was dominated by quartz and tiny amount muscovite and chlorite.

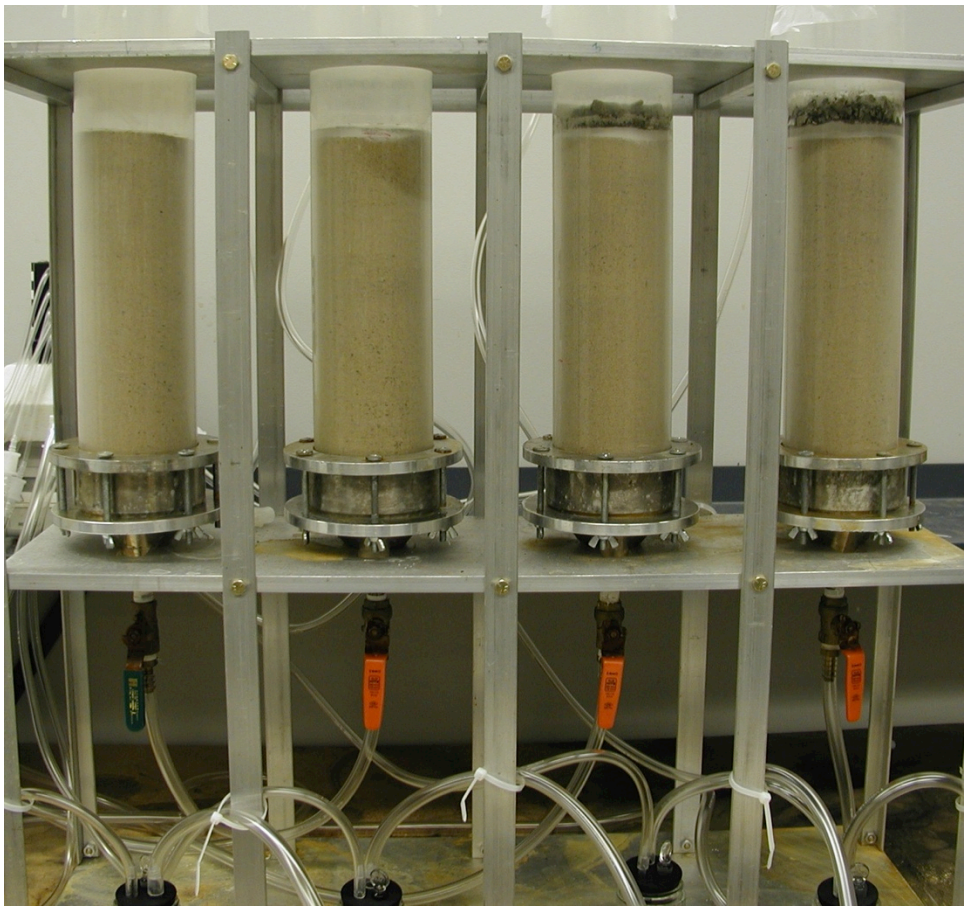

Figure 2-2. Column setups from left to right: 1) FW (10” FW soil), 2) FWAs (10”FW soil + 1/6” As_2O_3), 3) FWAsG (10” FW soil + 1/6” As_2O_3 + ½”gravel), 4) FW2AsG (10” FW soil + 1/3” As_2O_3 + ½” gravel).

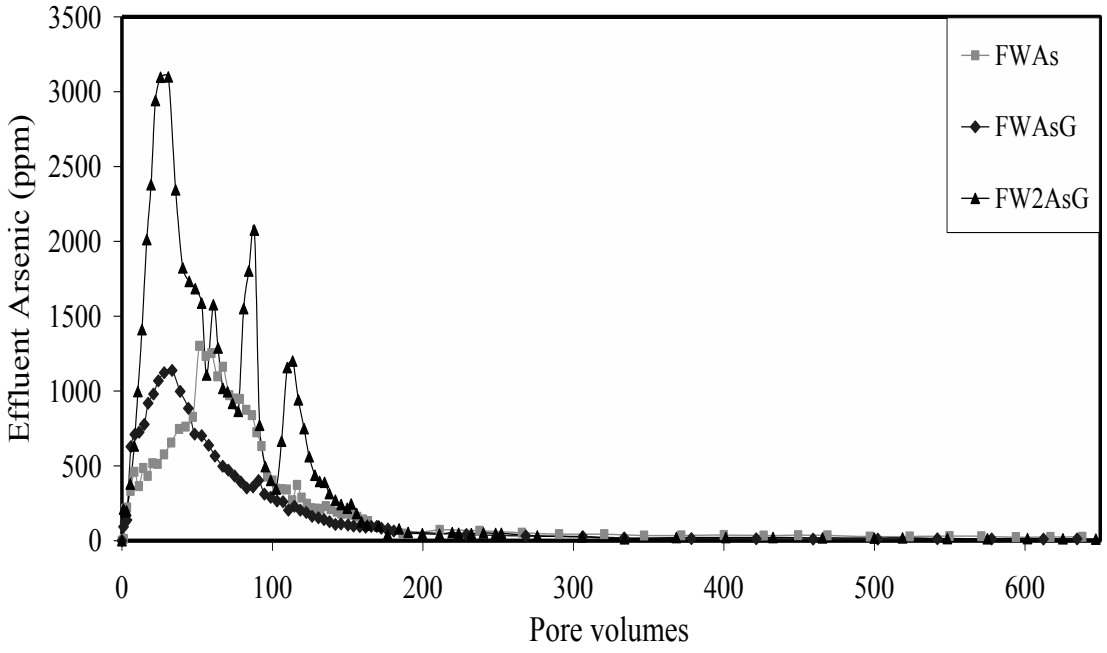

Figure 2-3. Total arsenic release from the spiked columns. Note the later arsenic peak for the ungraveled column (FWAs) and the significantly higher arsenic peak for the doubly spiked column (FW2AsG).

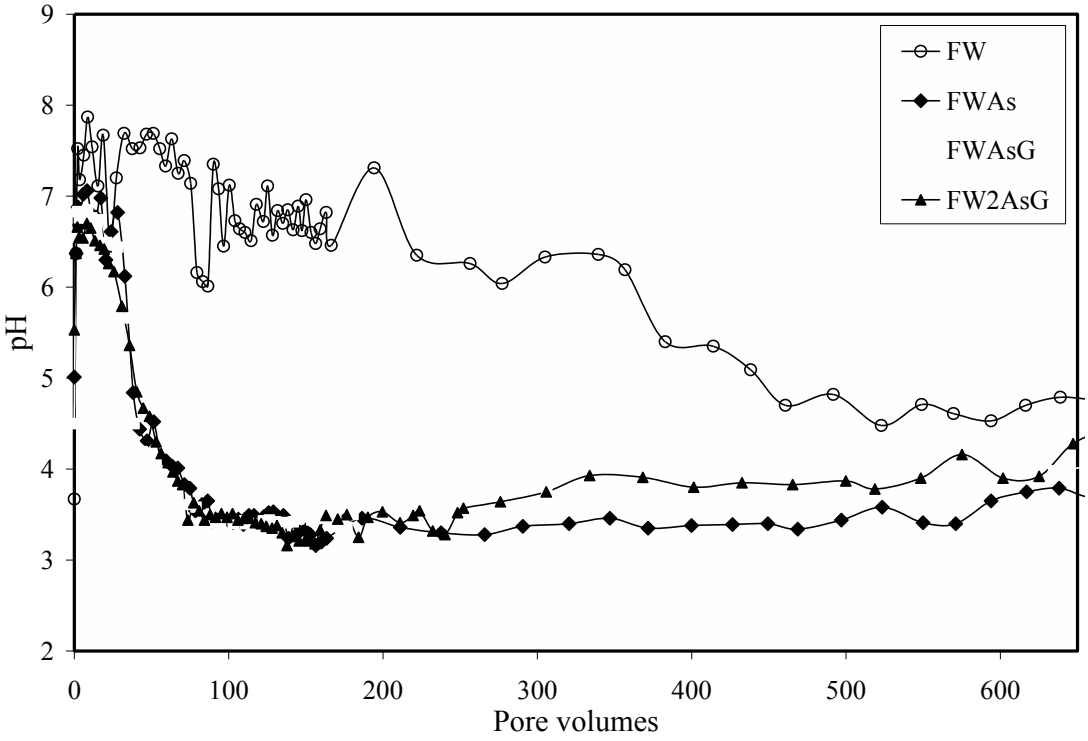

Figure 2-4. Changes in column effluent pH during leaching.

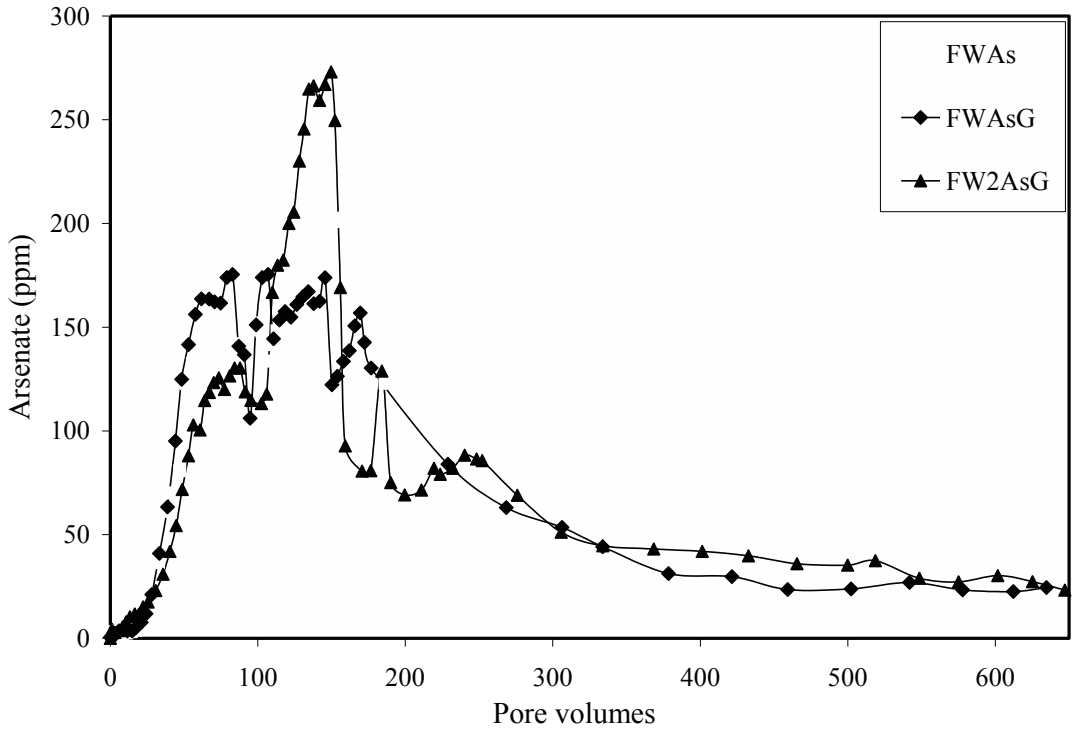

Figure 2-5. Column effluent arsenate concentration changes with pore volume for the three spiked columns.

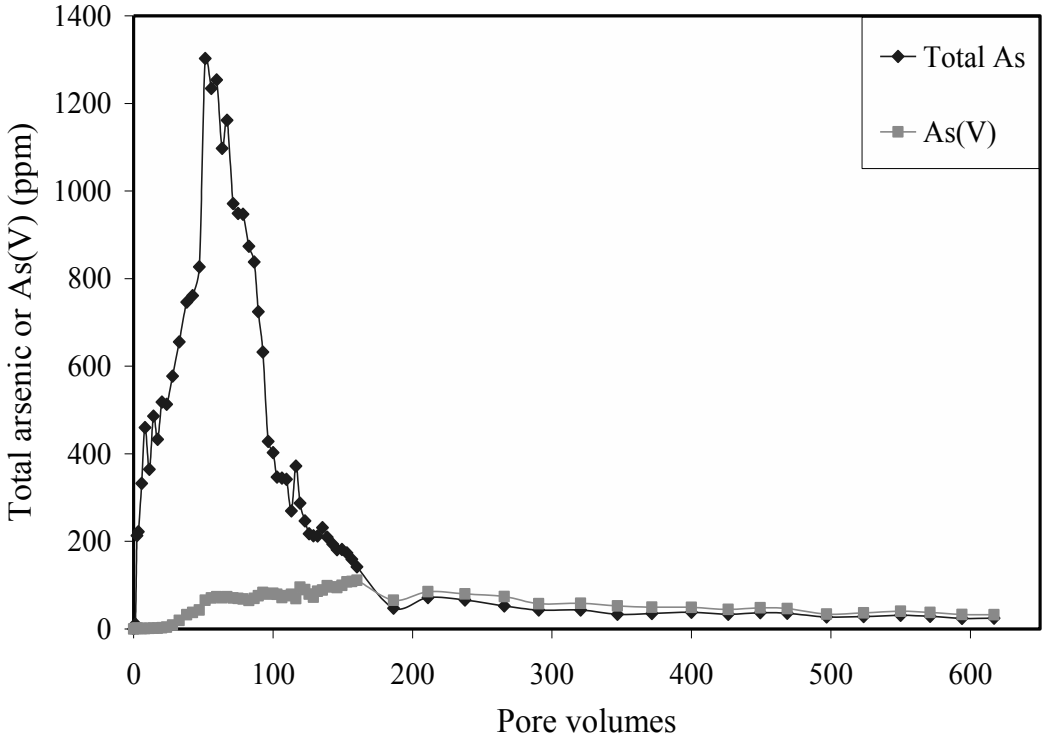

Figure 2-6. Comparison between total arsenic and As(V) in effluents of column FWAs.

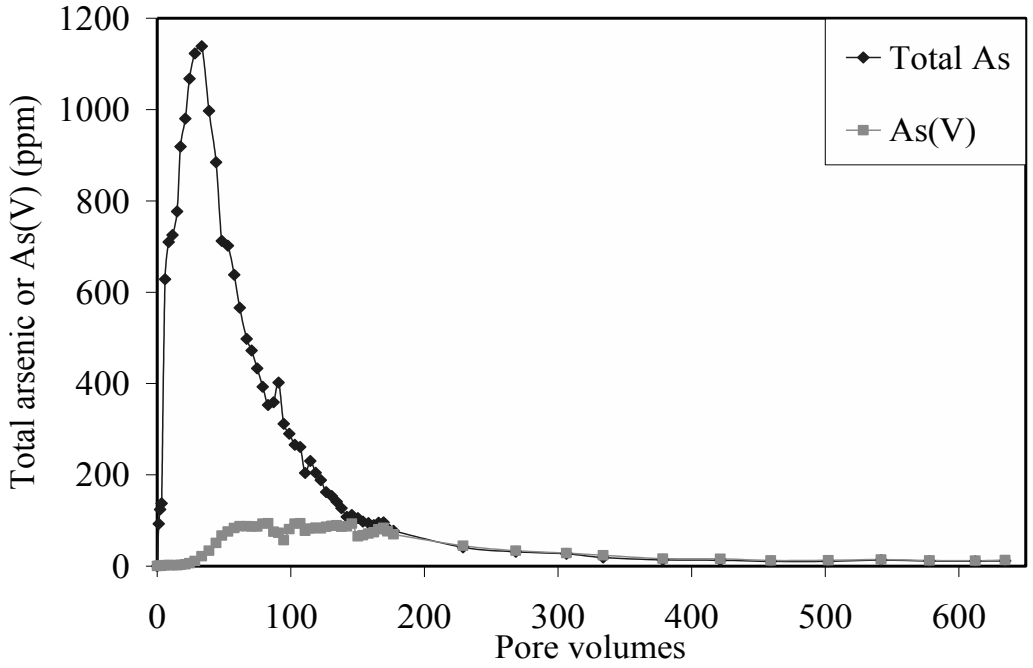

Figure 2-7. Comparison between total arsenic and As(V) in effluents of column FWAsG. 4.2. Eh-pH diagram

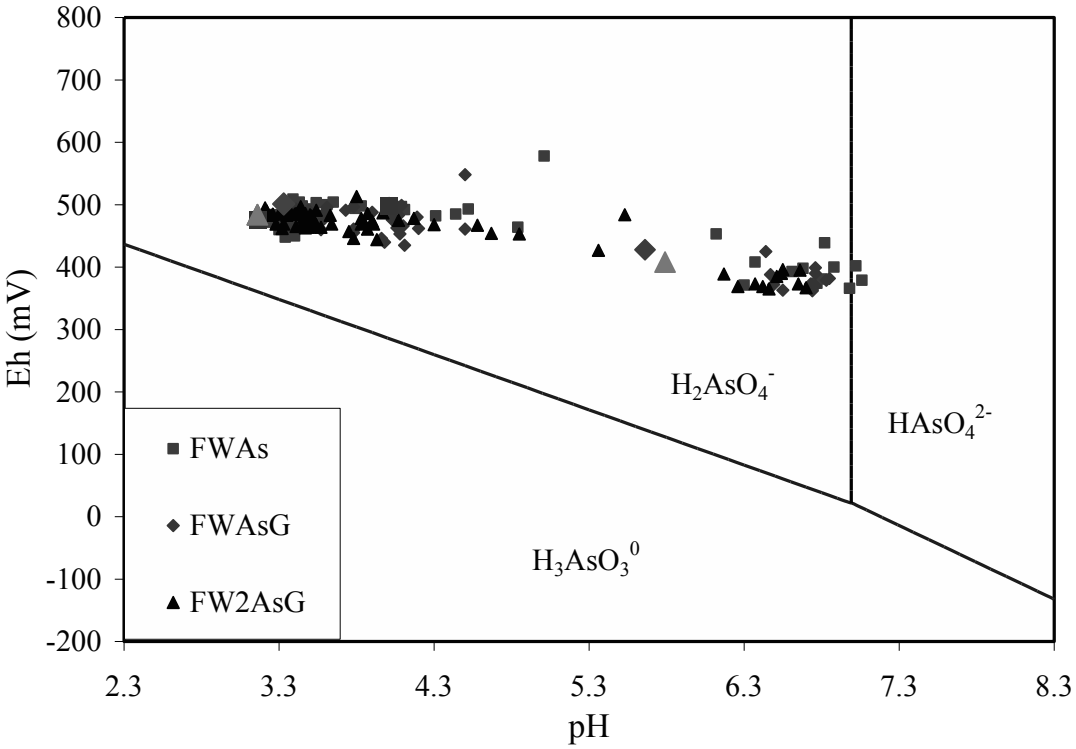

Figure 2-8. Distribution of arsenic species in effluent samples. Large symbols on the left and right indicate column effluent samples with peak arsenate and arsenic concentrations, respectively. Diagram constructed using thermodynamic data given by Nordstrom & Archer (2003).

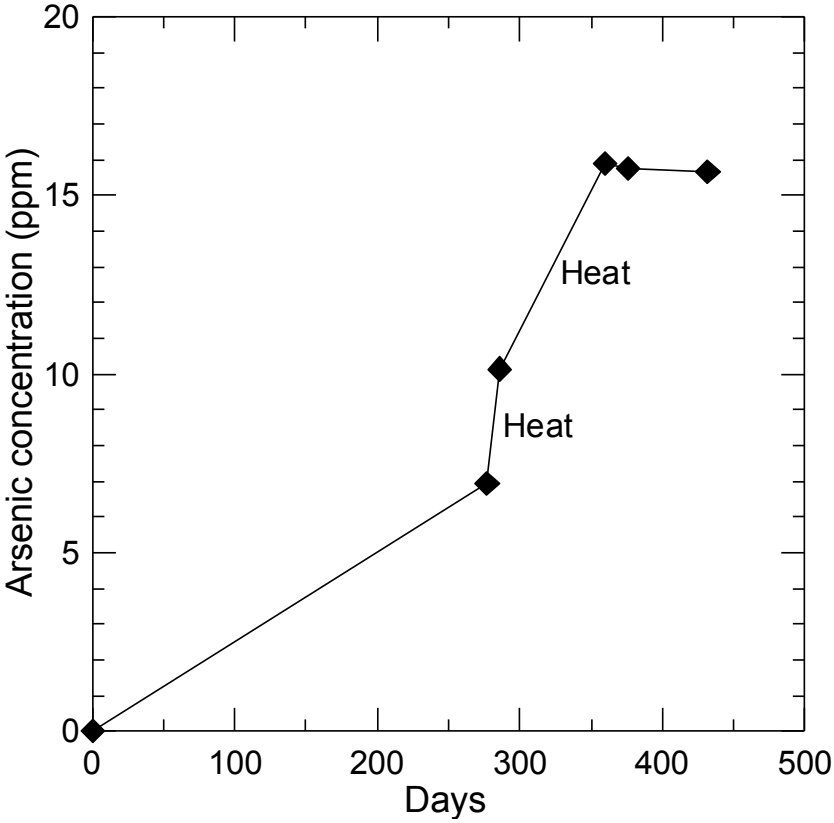

Figure 2-9. Arsenic trioxide dissolution curve with time.

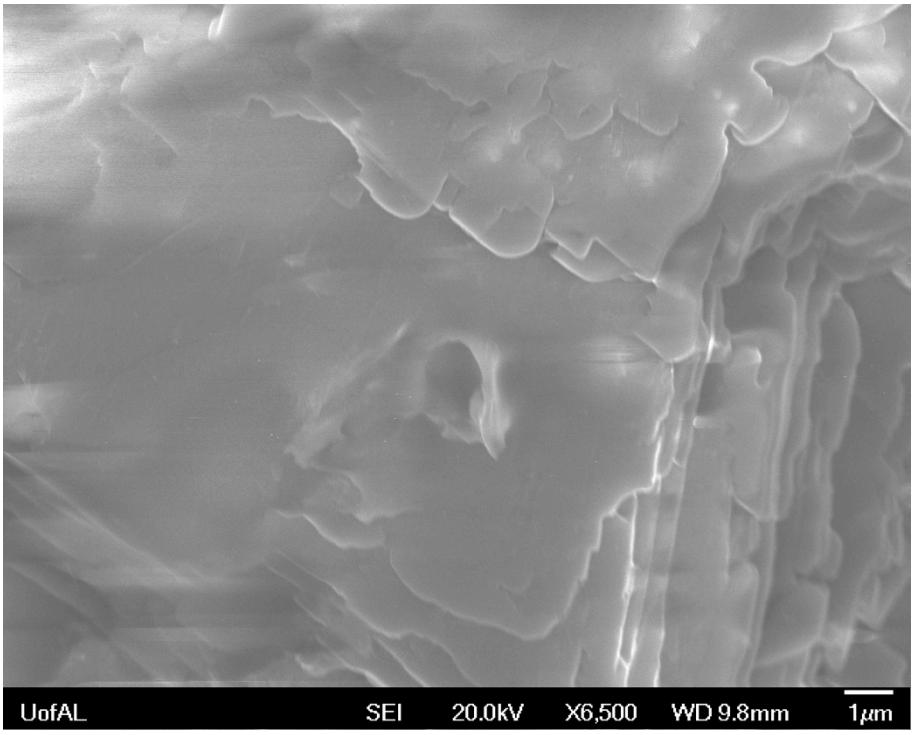

Figure 2-10. SEM image of arsenic trioxide residue from the top of column

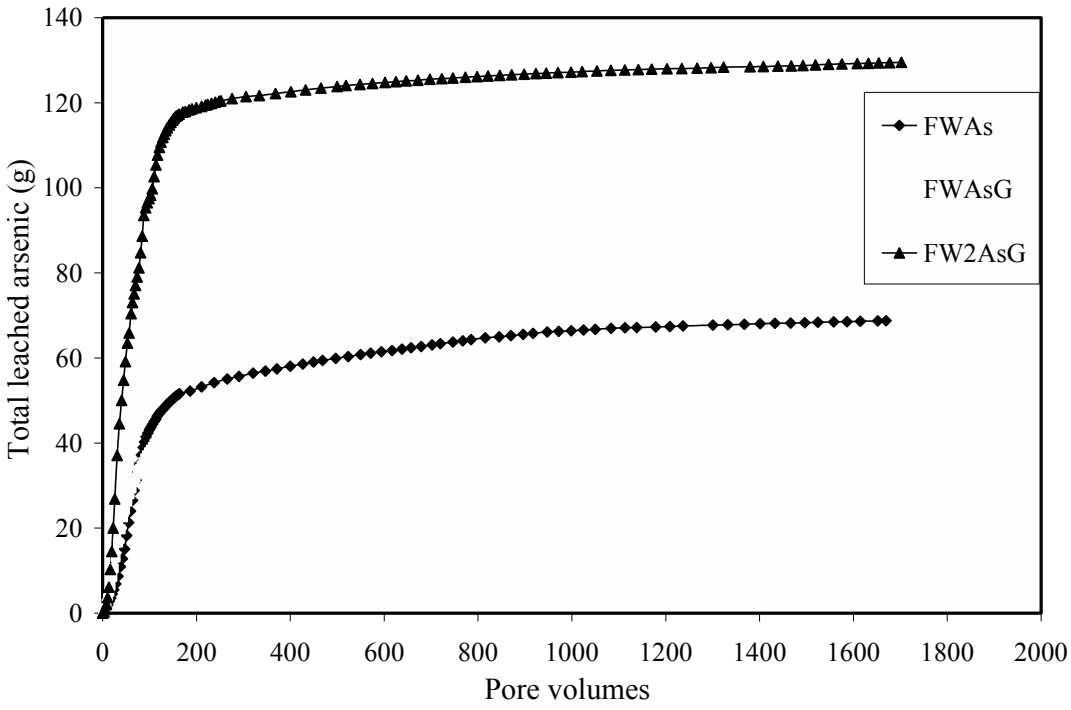

Figure 2-11. Arsenic leached from the spiked columns.

CHAPTER 3

MECHANISM OF ARSENITE OXIDATION IN SOIL COLUMN EXPERIMENTS

Abstract

After application of arsenic trioxide herbicide at Fort Walton site for 50 years, solid arsenic speciation study on the FW contaminated soil showed only As(V) there (Yang & Donahoe, 2007). It was not known the oxidation of As(III) to As(V) occurred during the contamination process or during the 50 years after. Further experimental simulation of arsenic trioxide leaching on the FW site showed As(III) dominated the initial arsenic release peak for the first 180 pore volumes. After 180 pore volumes, As(V) dominated the effluents. Complete oxidation of 60 mg/L of As(III) within the solution residence time in columns was an abnormally fast oxidation rate comparing to the inorganic As(III) oxidation rate. To further examine the arsenite oxidation mechanism, two series of serum bottle experiments were conducted. The results showed that arsenite was only oxidized in the nonsterile series, while oxidation was not observed for the autoclaved series. The experiments demonstrated that microbes were responsible for the observed arsenite oxidation. A total of 13 bacterial isolates were obtained from the reacted column soil and identified as *Burkhoderia fungorum* and *Burkhoderia* sp. (nov. proposed). These isolates were tested and shown to be efficient arsenite oxidizers. Finally, a comprehensive effort was made to construct a As(III) oxidation rate with initial As(III) concentration curve.

Keywords: Arsenite oxidation, bacteria, *Burkhoderia fungorum*, arsenite oxidase

1. Introduction

Arsenic trioxide herbicide application at Fort Walton site in 1950-60s led to soil arsenic contamination on the site. Solid arsenic speciation study showed arsenic in the soil was As(V) (Yang & Donahoe, 2007). Column experiments that simulated the arsenic contamination process showed As(III) dominated arsenic release peaks before 180 pore volumes, while As(V) dominated the arsenic contaminant tail after 180 pore volumes (Yue & Donahoe, 2009). Detailed analysis of the arsenite oxidation rate indicated the oxidation rate was contradictory to theoretical arsenite oxidation rate in water (Eary & Schramke, 1990), and hence, abnormal. Oxidation of arsenite by molecular oxygen is slow, with an arsenite half-life of c.a. one year in water open to the air (Eary & Schramke, 1990). The highest arsenite oxidation rate observed in the column was 22.5 mg/(L·h) As at pH 3.2; after 200 pore volumes, complete oxidation of As(III) to As(V) (60 mg/L tail) occurred within the 6.5 hour solution column residence time. This is comparable to the As(III) oxidation rate of 29 mg/(L·h) As at pH 7 in soil perfusion experiments (Quastel & Scholefield, 1953).

To understand the mechanism of the abnormally rapid arsenite oxidation rate, a serum bottle experiment was designed to differentiate microbial from abiotic oxidation. Then the oxidation mechanism was further characterized by isolating the arsenite oxidizing bacteria.

2. Materials and methods

2.1. Soil column experiments

Background soil FW was taken from the Fort Walton site, the soil was yellow sandy loam, composed of 99% quartz and tiny amount of chlorite and muscovite. The experimental setup is shown Figure 3-1. It included 4 soil columns: Column 1, or FW, only contained 10 inch FW soil, serving as a control. Column 2, or FWAs, contained 10 inch FW soil, plus 1/6 inch As_2O_3, serving to check As_2O_3 leaching behavior. Column 3, or FWAsG, contained 10 inch FW soil plus 1/6 inch As_2O_3 and ½ inch carbonate gravel, serving to check the influence of carbonate gravel, which was on the site. Column 4, or FW2AsG, contained 10 inch FW soil plus 1/3 inch As_2O_3 and ½ inch carbonate gravel, serving to check the influence of As_2O_3 layer thickness, and was described in Yue & Donahoe (2009). The results of the experiments are shown in Figure 3-2.

2.2. Serum bottle experiments

Two series of serum bottle experiments were conducted to determine the mechanism of arsenite oxidation in the column experiments. Both series (60 g soil + 60 g 350 mg/L As(III); 55 g soil + 60 g 350 mg/L As(III)) were sterilized by autoclaving, and then one series (with 55 g soil) was inoculated with unsterilized soil (5 g soil), while the other series was autoclaved with the soil already added. The bottles were opened to air for 10 minutes every day to maintain aerobic conditions, and a bottle from each series was sacrificed for both anion and cation analyses every other day over a 20-day period.

2.3. Isolation and identification of bacteria from reacted column soil

Arsenite oxidizing bacteria were isolated from the reacted column soils following the protocol of Suttigarn et al. (2005), and the isolates were identified by DNA extraction and sequencing as follows. A sterile toothpick was used to transfer bacteria from the colony on the agar plate to an autoclaved tube containing 50 μL autoclaved DDI water. After heating the tube at 100˚C for 0.25-3 hours, the tube was centrifuged for 1 minute to separate the cell fragments to the bottom, and 1 μL of the supernatant was withdrawn to measure its DNA concentration. If the DNA concentration was between 30 to 60 ng/μL, 1 μL of the supernatant solution was used for polymerase chain reaction (PCR) to amplify its 16S rDNA. The following primers were used: 8F: 5'-AGAGTTTGATCMTGGCTCAG-3'; 1525R: 5'-AAGGAGGTGWTCCARCC-3'. The PCR was conducted at the Molecular Systematics Facility at the University of Alabama. The PCR product was sent to OPERON company for sequencing commercially. After the DNA sequences were obtained, they were aligned using the BioEdit software and blasted at the NCBI Website and matched in the RDP database to obtain the best match with known bacterial strains.

2.4. Characterization of arsenite oxidizers and their oxidase

To test whether a bacterial strain could oxidize arsenite, 10 mg of biomass were taken from a colony on an agar plate, and homogeneously suspended in 20 mL of 300 mg/L autoclaved As(III) solution at pH 6-7, The cell suspension was incubated at room temperature for two days, and the pH of the suspension was checked after filtration through a 0.2 μm syringe filter. A significant pH drop (e.g,, >1 pH unit) indicated As(III) oxidation. The reaction for the test was: $2As(OH)_{3(aq)} + O_{2(aq)} = 2H_2AsO_4^- + 2H^+$. To compare the oxidizing capabilities of different arsenite oxidizing bacteria, different oxidizing strains were inoculated on the same plate and incubated at 25℃ for three days. Biomass samples of 26 mg were taken for each species and

made into 110 μL suspensions with autoclaved DDI water. A 10 μL aliquot of the cell suspension was taken and spiked into each vial containing 10 mL of ~380 mg/L As(III). A series of 10 replicate vials was created for each oxidizing strain of bacteria. The sample sacrifice schedule was same as for the serum bottle experiments.

The arsenite oxidase gene was amplified using the following primers: aoxBM1-2F: 5'-CCACTTCTGCATCGTGGGNTGYGGNTA-3' and aoxBM3-2R: 5'-TGTCGTTGCCCCAGATGADNCCYTTYTC-3' (Quéméneur et al., 2008). After the gene sequence was obtained, it was converted to an amino acid sequence using the BioEdit software. Cell motility was checked, as described in Skerman (1967).

3. Results

3.1. Serum bottle experiments

IC analysis of As(V) of the aqueous solutions showed increasing arsenate concentrations with time in the inoculated non-sterile series, but no oxidation occurred in the sterile series during the same period (Figure 3-4). This indicated that the arsenite oxidation observed in both the column and serum bottle experiments was caused by microbes. ICP-OES analysis of total arsenic of the aqueous samples showed decreasing trend with time in both the sterile series and non-sterile series. These trends were caused by arsenic adsorption onto soil mineral surfaces.

3.2. Arsenic-resistent bacteria isolated from reacted soil columns

Thirteen isolates were obtained from the column soil; the isolates were identified by 16S rDNA sequencing: 11 (A1=A2=A3=A6=A7=A8=A9=A10=A11=A12=A13, referred as strain

A12 after) belonged to *Burkholderia fungorum* LMG 16225^T (100% match) and 2 (A4=A5, referred as strain A4 after) belonged to *Burkholderia* sp. The latter was closest to *B. zhejiangensis* CCTCC AB 2010354^T and *Burkholderia glathei* DSM 50014^T, with similarities of 99.1% and 97.3%, respectively, based on 1441 base pairs of 16S rDNA sequence. Further effort to isolate arsenite-oxidizing or arsenite-resistant bacteria from the columns also produce *Bacillus* species.

All the soil isolates were tested for their As(III) oxidizing capacities. The results showed both strains A4 and A12 could oxidize As(III) to As(V). Further kinetic studies showed strain A12 was the more efficient oxidizer, oxidizing arsenite efficiently at pH as low as 2.5, while the oxidation efficiency of strain A4 was lower at initial (first day) and final stage after the third day or pH<3, or As(V) $\geq$ 150 mg/L (Figure 3-6).

3.3. Bacterial arsenite oxidation rate as a function of different initial As(III) concentrations

Figure 3-8 shows that the arsenite oxidation capability of strain A12 fluctuated with initial As(III) concentrations for a 4-day oxidation period open to the air. At low initial As(III) concentration of 130 mg/L, As(III) was completely oxidized. When the peak As(V) concentration of approximately 400 mg/L was reached for an intital As(III) concentration of 600 mg/L. When the initial As(III) concentration exceeded 2300 mg/L, the arsenite oxidation capability remained low (less than 39 mg/L As(V)) Figure 3-8). In the column experiments, only column FW2AsG, which simulated the maximum herbicide application, had a short period when the effluent As concentration exceeded 2300 mg/L. The bacterial arsenite oxidation capacities of columns FWAs and FWAsG would fall on the high plateau area of Figure 3-8.

Both strain A4 and strain A12 are non-motile bacteria, which made it difficult to see any activity changes at high As(III) concentrations. Therefore, to check the activity of bacterial cells at very high As concentrations, the motility of *Burkhoderia glathei* DSM 50014^T, which was also tested as arsenite oxidizing, was checked at As(III) concentrations in the column experiments and up to As_2O_3 saturation (~1.8% As(III)). The results showed *Burkhoderia glathei* DSM 50014^T kept motile t 4,000 mg/L As(III), but lost motility at As_2O_3 saturation. These cells at As_2O_3 saturation, including strains A4 and A12 could survive for at least 10 days, but survival rate was unknown. After several months, no cell was tested to survive from such concentrated As(III) solution on nutrient agar plate.

3.4 Arsenite oxidase

Bacterial arsenite oxidase was detected by DNA sequencing in both strains A4 and A12. The sequences were converted into amino acid sequences and compared between strains A4 and A12 (Figure 3-7). Arsenite oxidase consists of a large Mo-pterin subunit (aoxB) and a small Fe-S Rieske subunit (aoxA) (Silver & Phung, 2002; 2005). Figure 3-7 shows partial sequences of aoxB for both strain A4 (*B. sp.*) and strain A12 (*B. fungorum*). The similarity of AoxB between strains A4 and A12 is 95%, which is the same as their 16S rDNA similarity. This is consistent with the established concept that arsenite oxidase is transmitted vertically and is very conserved (Lebrun et al. 2003). The AoxB partial sequences did not contain the functional group where at least two cysteine residues existed, but the detection of the arsenite oxidase gene supported the efficient oxidizing behaviors of strains A4 and A12.

4. Discussions

4.1 Bacterial As(III) oxidation curve

Figure 3-8 shows that the arsenite oxidation capacity of strain A12 changed with different initial As(III) concentrations. Because the oxidation time was 4 days for eachexperiment, the curve is easily converted to an oxidation rate vs. initial As concentration by dividing the arsenate concentrations by four days. By such conversion, the first point at the lowest initial As value is invalid. The experimental data show the strain A12 arsenite oxidation rate did not decrease at initial As(III) concentrations as low as 100 mg/L, compared to an initial As(III) concentration of 500 mg/L, and was even higher at 100 mg/L initial As(III). These points all fall on the arsenite oxidation plateau between 100 mg/L to ~1200 mg/L initial As.

Using the data shown in Figure 3-8, a bacterial As(III) oxidation rate curve was calculated for initial As(III) concentrations above 500 mg/L (Figure 3-10). This figure shows that the high oxidation rate plateau can be extended to an initial As(III) concentration of 100 mg/L by experimental results which showed that the bacterial As(III) oxidation rate did not decrease, but actually increased, for initial As(III) concentrations of 500 mg/L to 100 mg/L. The column experiment data shown in Figure 3-9a, b, c shows that once the effluent arsenic concentrations dropped below 50 mg/L, As(V) became the dominant arsenic specie in the effluents. This observation suggests that the oxidation rate producing 50 mg/L As(V) is still on the high oxidation plateau, and the plateau can therefore be extended to 50 mg/L initial As(III). It should be recognized that the calculated oxidation rates shown in Figure 3-10 are simply estimated values; measured oxidation rates would depend on biomass concentrations, analytical equipment precision, bacterial strain, etc. Despite this, the calculated bacterial oxidation rate curve is useful

because it shows a trend which is consistent with observations made during the column experiments.

4.2 Understanding the As(III) oxidation rate on a cellular scale

The bacterial As(III) oxidation rates calculated for construction of Figure 3-10 were independent of biological detail. In this section, these details are briefly explored. Bacterial cells have a density a little greater than that of water, so they tend to collect at the bottom of solution vessels or attach to solid surfaces. While the attachment to solid surfaces might have been important in the column experiments, the settling of cells likely applied to bacterial As(III) oxidation in the vial experiments shown in Figure 3-8. Both strain A4 and A12 have relatively small cell sizes and were therefore in constant Brownian motion. However, the speed of Brownian motion was much less than that of molecular movement (i.e., diffusion), which transported As(III) and molecular oxygen to the cell, so the cells can be considered immobile. Although Brownian motion of the cells was slow, it kept the cells dispersed to be available to As(III) and molecular oxygen by preventing the cells from clumping together. After As(III) and molecular oxygen reached a cell, they had to find specific transporters to enter the cell's periplasmic space. When As(III) entered the cell, it underwent rapid electron transfer by oxidase enzyme catalysis. Subsequently, the produced As(V) would be expelled from the cell, which would require energy for strains A4 and A12. While higher As(III) concentrations would enable As(III) to enter the cell more easily by diffusion; the lower observed oxidation rate indicated the bacterial cell might have protected itself by closing the transporters.

5. Summary and conclusions

The serum bottle experiments performed in this study indicated that microbial processes were responsible for the arsenite oxidation observed in the column experiments. Bacterial strains A12 and A4 were isolated from the reacted column materials and proven to be capable of arsenite oxidation. The method to test if a bacterial strain could oxidize arsenite by pH was one of the new contributions of this project. Strain A12 was a more efficient arsenite oxidizer than strain A4, especially below pH 3. Detection of arsenite oxidase supported an enzymatic oxidation pathway. Arsenite oxidation experiments conducted with strain A12 at different initial As(III) concentrations revealed that the bacterial arsenite oxidation rate decreased for initial arsenite concentrations >1200 mg/L, which is opposite from what would be expected for inorganic oxidation. By compiling this data, further experimental evidence, and column experiment data together, a calculated bacterial As(III) oxidation rate curve was constructed, which showed the oxidation rate trend with initial As(III) concentration. The calculated trend is consistent with the column experiment observations, but is independent of biomass concentrations and therefore not defined by the values on the vertical axis. The calculated bacterial As(III) oxidation curve was based on the As(V) analytical data, independent of biological detail. Exploration of the bacterial As(III) oxidation rate on a cellular scale improved our understanding of the oxidation mechanism operating in the soil column experiments.

Determination of bacterial arsenite oxidation in the column experiments provides insight into the arsenic contamination process at the field site. Because numerous studies (Quastel & Scholefield, 1953; Osborne & Ehrlich 1976; Philips & Taylor, 1976; Turner, 1949; Turner, 1954; Turner & Legge,1954; Suttigarn et al., 2005) have shown that bacterial arsenite oxidation used molecular oxygen as the oxidant, arsenite oxidation would be limited by oxygen availability at

the contaminated site. Oxygen availability will change with the season, due to the inverse relationship between temperature and oxygen solubility. Arsenite would have been the dominant arsenic species in the contaminant plume head until the arsenic trioxide leachability decreased arsenite concentrations to below the oxidizing capability of the soil bacteria. At that point, the contaminant plume tail would be dominated by arsenate and persist for decades. Whenever the plume head (arsenite) is exposed to the air (e.g., groundwater discharge or installation of tube wells), microbial arsenite oxidation would resume.

References

Eary, L. E., Schramke, J. A. 1990. Rates of inorganic oxidation reactions involving dissolved oxygen. pp. 379-396. In: Chemical modeling of aqueous systems II. Eds: D. C. Melchoir and R. L. Bassett. Washington DC, American Chemical Society.

Lebrun, E, Brugna,M, Baymann,F., Muller, D., Lie`vremont, D,, Lett, M.-C., Nitschke, W. 2003. Arsenite Oxidase, an Ancient Bioenergetic Enzyme. Molecular Biology and Evolution. 20(5):686–693.

Osborne, F. H., Ehrlich, H. L. 1976. Oxidtation of arsenite by a soil isolate of *Alcaligenes*. Journal of Applied Bacteriology. 41: 295-305.

Philips, S., Taylor, M. 1976. Oxidation of arsenite to arsenate by *Alcaligenes faecalis*. Applied and Environmental Microbiology. 32(3): 392-399.

Quastel, J. H., Scholefield, P. G.1953. Arsenic oxidation in soils. Soil Science. 75: 279-285.

Quéméneur, M., Heinrich-Salmeron, A., Muller, D., Lièvremont, D., Jauzein, M., Bertin, P. N., Garrido, F., Joulian, C. 2008. Diversity surveys and evolutionary relationships of *aoxB* genes in aerobic arsenite-oxidizing bacteria. Applied Environmental Microbiology. 74**:**4567-4573.

Skerman, V. B. D. 1967. A guide to the identification of the genera of bacteria, 2nd edn. Baltimore: Williams & Wilkins.

Silver, S., Phung, L. T., Rosen, B. P. 2002. Arsenic metabolism: resistance, reduction, and oxidation. pp. 247-272. In: Environmental Chemistry of Arsenic. W. T. J. Frankenberger. New York, Marcel Dekker, Inc.

Silver, S., Phung, L. T. 2005. Genes and enzymes involved in bacterial oxidation and reduction of inorganic arsenic. Applied and Environmental Microbiology. 71(2): 599-608.

Suttigarn, A., Wang, Y. T., Asce, M. 2005. Asenite oxidation by *Alcaligenes faecalis* strain O1201. Journal of Environmental Engineering. 131(9): 1293-1301.

Thompson J. D., Higgins D. G., Gibson T. J. 1994. CLUSTAL W: improving the progressive multiple sequence alignment of sequence weighting, position specific gap penalties and weight matrix choice. Nucleic Acids Research. 22: 4673-4680.

Turner, A. W. 1949. Bacterial oxidation of arsenite. Nature. 164, 76-77

Turner, A. W. 1954. Bacterial oxidation of arsenite. I. Description of bacterial isolated from arsenical cattle-dipping fluids. Australian Journal of Biological Science. 7, 452-478.

Turner, A. W., J. W. Legge, 1954. Bacterial oxidation of arsenite. II. The activity of washed suspensions. Australian Journal of Biological Science. 7, 479-495.

US EPA, 1994. Method 1312: Synthetic Precipitation Leaching Procedure. In: US Environmental Protection Agency, Office of Solid Waste, Test Methods for Evaluating Solid Waste, Physical/Chemical methods, 3rd ed., Washington, DC: US Government Printing Office.

Yang, L., Donahoe, R. J., 2007. The form, distribution and mobility of arsenic in soils contaminated by arsenic trioxide, at sites in southeast USA. Applied Geochemistry. 22, 320-341.

Yue, Z., Donahoe, R. J. 2009, Experimental simulation of soil contamination by arsenolite. Applied Geochemistry. 24(4): 650-656.

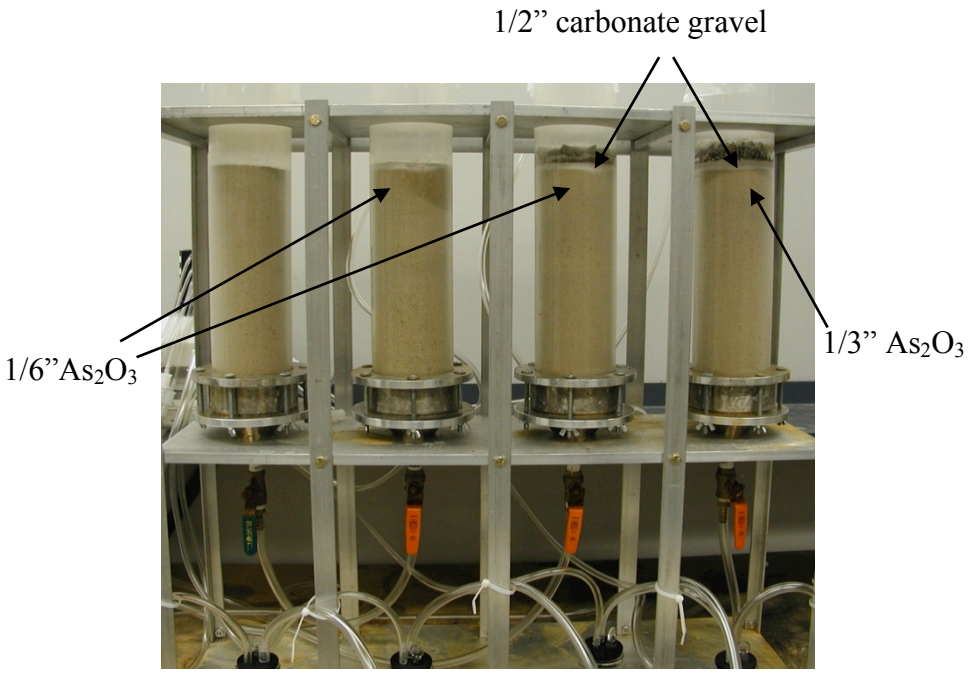

Figure 3-1. Column experimental setup. From left to right: 1) FW (no As spike); 2) FWAs; 3) FWAsG; 4) FW2AsG. Synthetic precipitation was applied to column tops and effluent samples were collected at the bottoms of the columns. The effluents were analyzed by ICP-OES and IC for total As and As(V), respectively

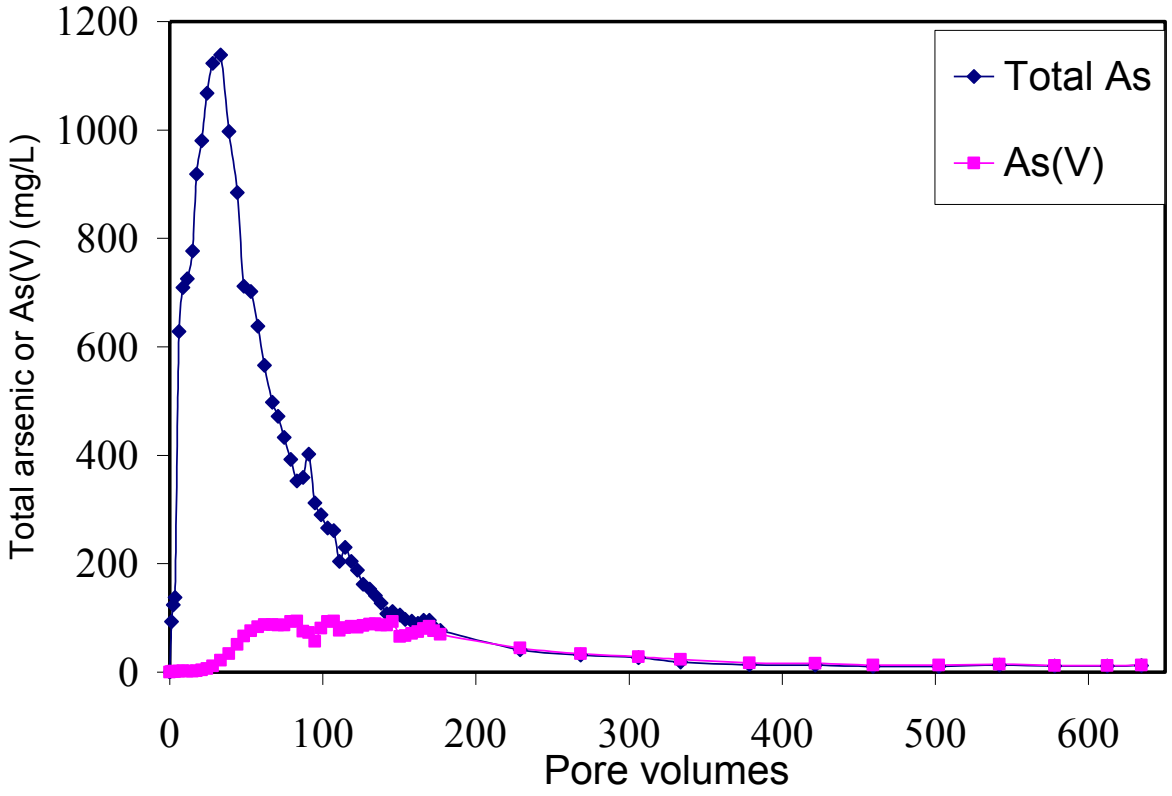

Figure 3-2. Column effluent solution arsenic concentrations. Only data from column 3 are shown, Data from columns 2 and 4 were similar to column 3

Figure 3-3. Serum bottle setup: 60 g soil + 60 g 350 mg/L As(III) solution with ~60 mL headspace.

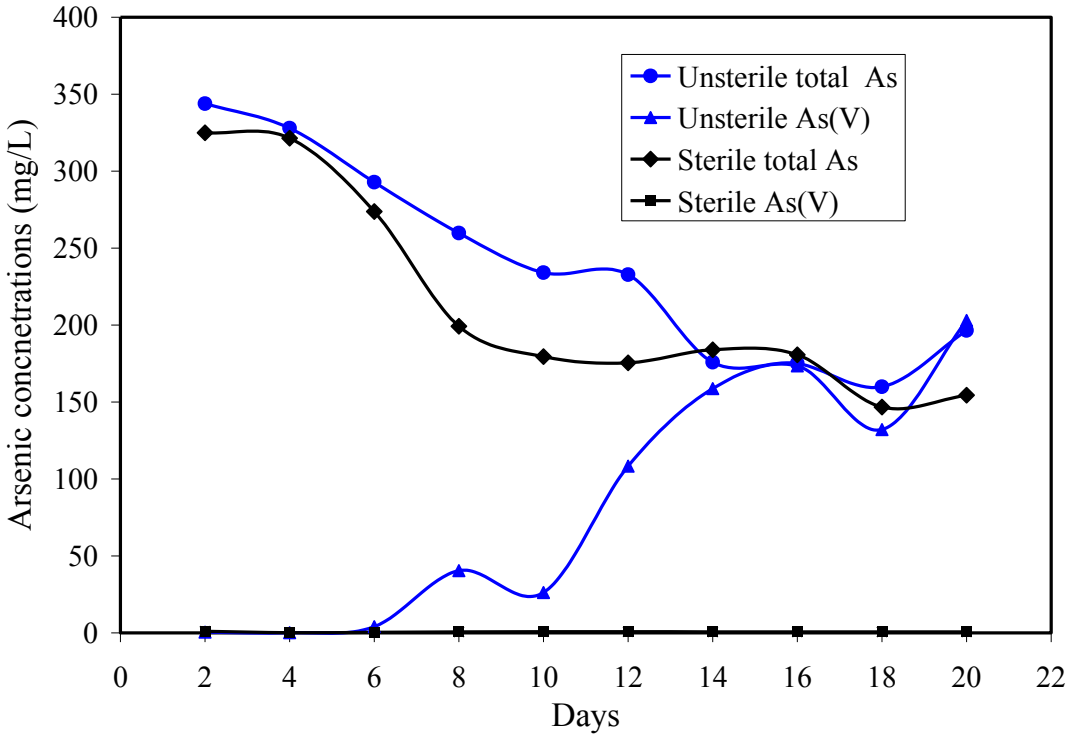

Figure 3-4. Serum bottle experiment results. Only the inoculated (unsterile) series showed increase in arsenate concentration with time.

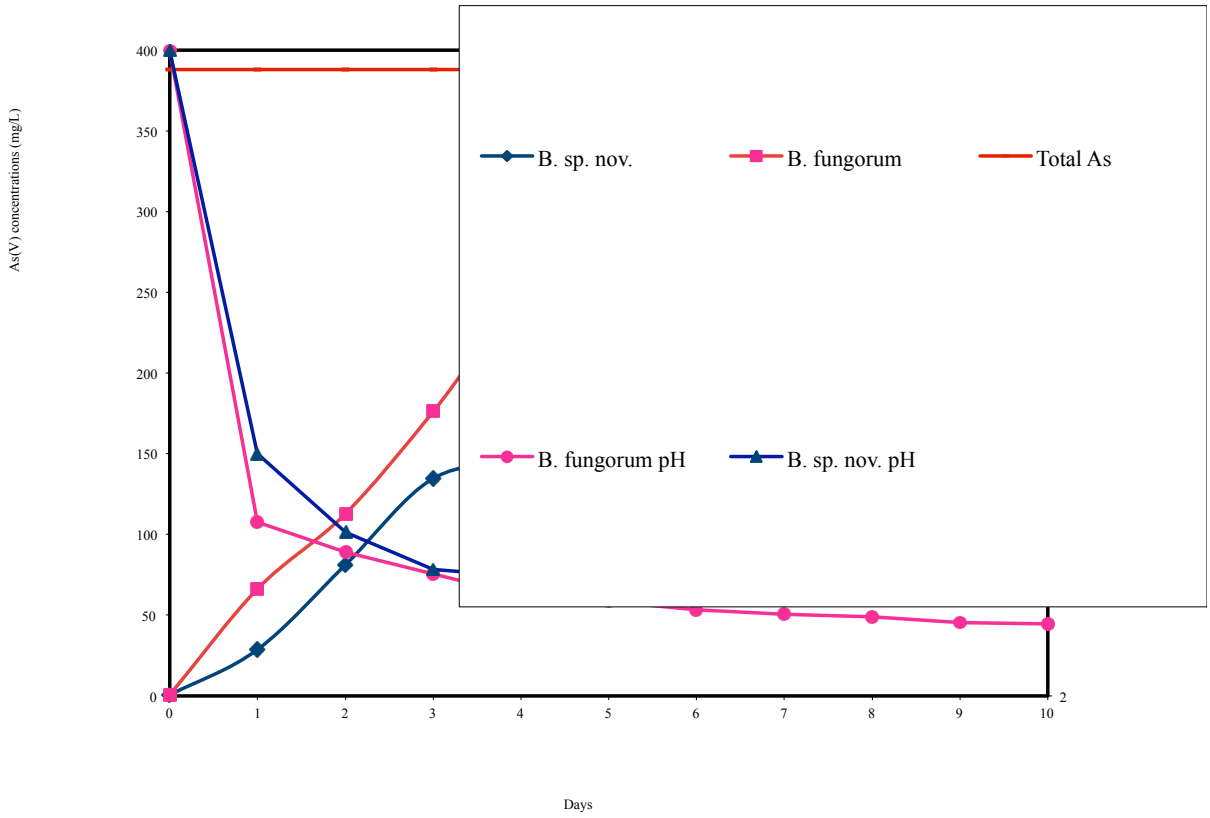

Figure 3-5. Arsenite oxidation kinetic curve for *B. fungorum* and *B.* sp.

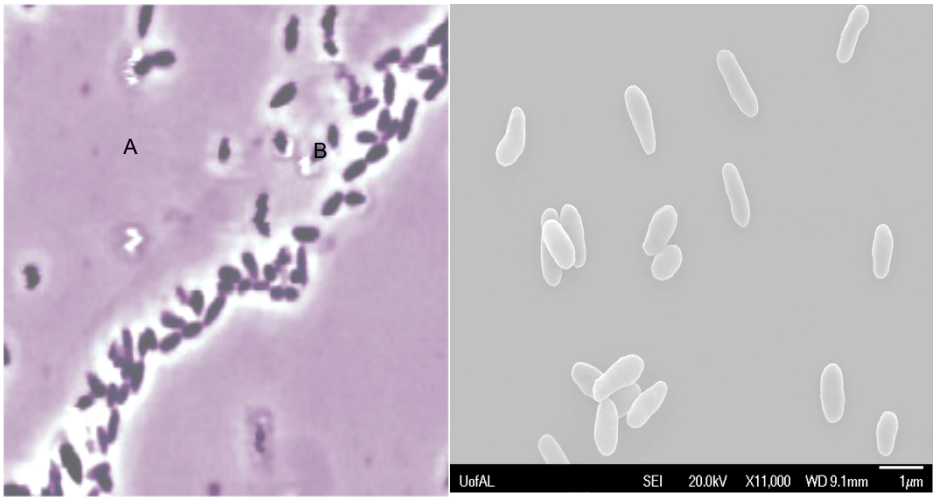

Figure 3-6. Arsenite-oxidizing species from the soil column: *Burkholderia fungorum* (A) and *Burkholderia* sp. (nov. proposed) (B)

A13:ALGLDYNKQLPPMAVTLTPAMTNVVTDRDGSRHRIMIVPDRECVVNSGLSS

A4: ALGLDYNKQLPP LA IXLTPAMTNVVTDRDGSRHRIMIVPDRECVVNSGLSS

TRGGKMASYMYNADGLTRDRLKNPRLYVGDQWVDTDWDHAMAIYAGLL

TRGGXMATYMYDADGLTRERLKNPRLYAGDQWVDTDWDHAMAIYAGLL

KRTLDKDGPNGIVFSAFDHGGAGGGFENTWATGKLMFTALQTPMVRIHNRPAY

KRTLDKDGPNGI IFSAFDHGGAGGGFENTWATGKLMFTAL KTPMVRIHNRPAY

NSECHATREMGIGELNNSYEDAELADVIMAVGNNAYETQTNYF

NSECHATREMGIGELNNSYEDAELADVIMA IG NNAYETQTNYF

LNHWVPNLQGGTAEKKKQRFAGEATPATRIIFVDPRRTPTIAIAEQVAGAGNVL

LNHWVPNLQGGTAQKKKQRFAGEATPATRIIFVDPRRTPTIAIAEQVAGAGNVL

HLDILPGTDVALFNGLFTYVVEQGWIDRDFINQHTNGFDDAVKTN

HLDILPGTDVALFNGLFTHVVEXGWIDRDFINQHTNGFDDAVKTN

Figure 3-7. Comparison between strain A4 (*B. sp.*) and strain A12 (*B. fungorum*) arsenite oxidase aoxB sequences.

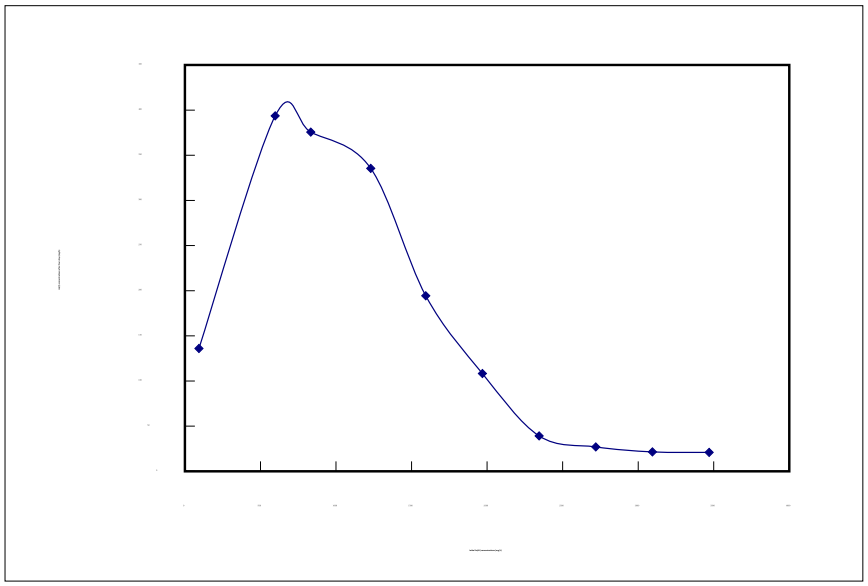

Figure 3-8. Arsenite oxidation capability with different initial arsenite concentrations. Around 10 mg A12 wet biomass/20mL As(III) solution at room temperature.

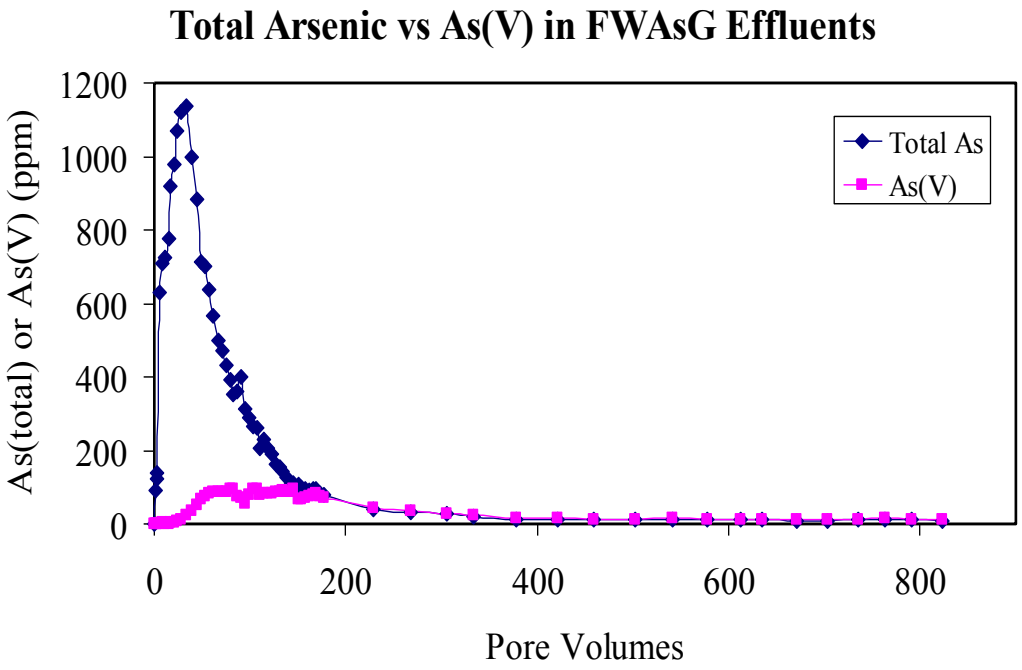

Figure 3-9a.Total arsenic vs. A(V) in columns FWAsG.

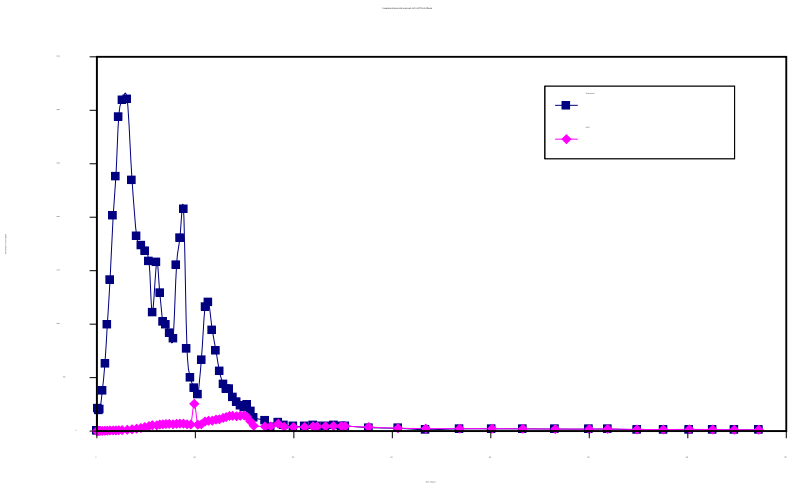

Figure 3-9b.Total arsenic vs. A(V) in column FW2AsG.

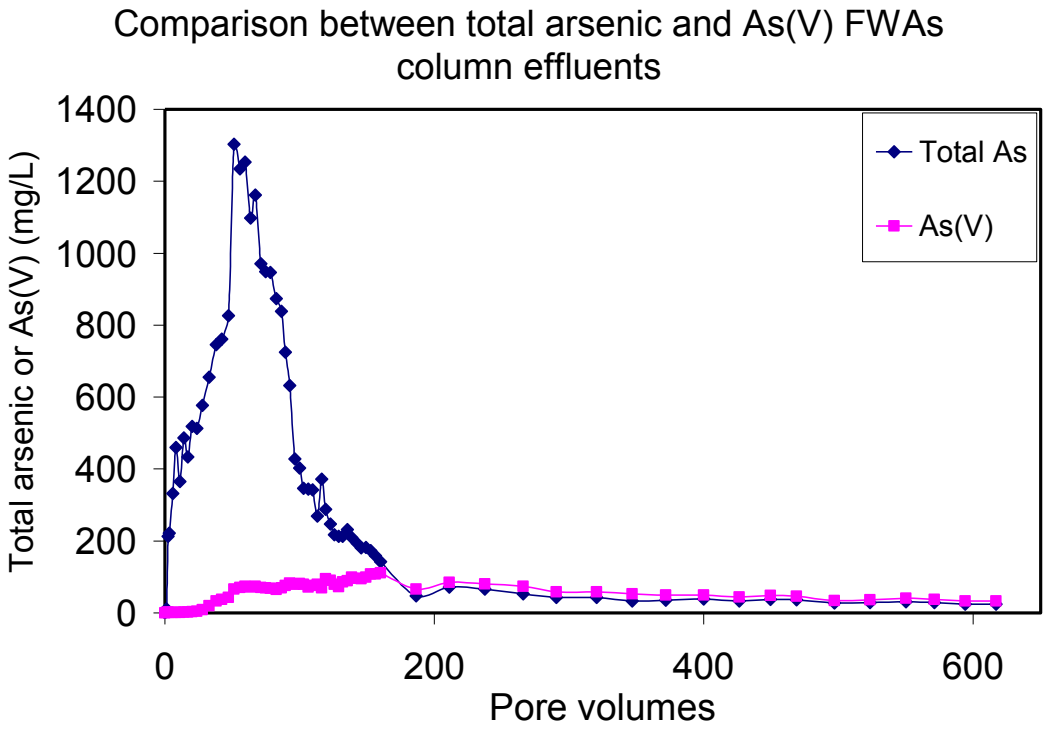

Figure 3-9c.Total arsenic vs. A(V) in column FWAs.

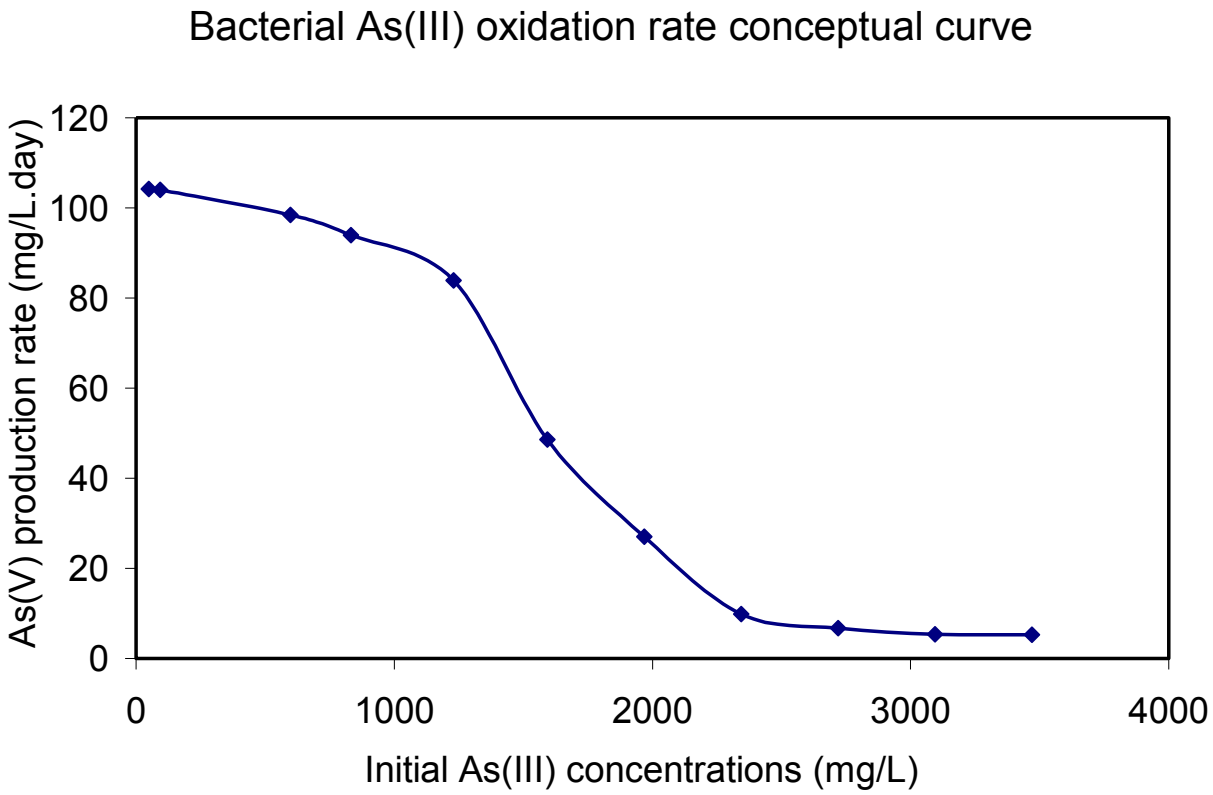

Figure 3-10 Bacterial As(III) oxidation rate conceptual curve.

CHAPTER 4

BURKHOLDERIA ARSENICOXYDANS SP. NOV., AN ARSENITE OXIDIZING BACTERIUM FROM ARSENIC TRIOXIDE-CONTAMINATED SOIL

Abstract

An arsenite-oxidizing bacterium strain A4, isolated from arsenic trioxide-contaminated soil, was subject to polyphasic characterizations to determine its taxonomic position. Strain A4 were aerobic, Gram negative, and non-motile short rods or ovoids with soma size measuring 0.3-0.6×0.5-3.5 μm. Catalase and oxidase were positive. Its major polar lipids included 18:1 7ω7c, 16:0, summed feature 3, 17:0 cyclo, and its polar lipids pattern was similar to other *Burkholderia* species. Its major polar lipids included PE1, PE2, PG, and an unknown phospholipid. Its predominant respiratory quinone was ubiquinone-8. Its genomic DNA G+C content was 63.5 mol%. Its closest relatives, according to 16S rDNA sequences, were *Burkholderia zhejiangensis* CCTCC AB 2010354^T, *Burkholderia glathei* DSM 50014^T and *Burkholderia sordidicola* KCTC 12081^T with similarities of 99.1%, 97.3% and 96.7%, respectively. Its 16S rDNA similarities with all other type strains in the genus *Burkholderia* were all below 96.5%. DNA-DNA hybridization between strain A4 and *Burkholderia glathei* DSM 50014^T showed their DNA-DNA relatedness was 49% or lower. Based on this data genomic data of *Burkholderia zhejiangensis* CCTCC AB 2010354^T, strain A4 represents a novel species in the genus *Burkholderia*, for which the name *Burkholderia arsenicoxydans* was proposed. The type strain is A4^T (= ATCC BAA-2404^T =CCTCC AB 2012027^T).

Keywords: Arsenite oxidizng, *Burkhoderia arsenicoxidans* sp. nov.

1. Introduction

In an effort to search for arsenite oxidizers to understand the mechanism of arsenite oxidation in soil column experiments (Yue & Donahoe, 2009), two strains (A4 and A12) of bacteria were isolated as arsenite oxidizers from the column materials. Strain A12 was found to belong to *Burkholderia fungorum* LMG 16225^T (100% match of 16S rDNA sequence), and strain A4 was closest to *Burkholderia zhejiangensis* CCTCC AB 2010354^T and *Burkholderia glathei* DSM 50014^T with 16S rDNA sequence similarities of 99.1% and 97.3% respectively. A polyphasic characterization, including phenotypic and biochemical characterization, 16S rDNA sequence analysis, DNA-DNA hybridization, and fatty acids analysis, was conducted on strain A4 to determine its taxonomic position. The results suggested A4 represented a novel species of the genus *Burkholderia*.

The genus *Burkholderia* was created by Yabuuchi et al. (1992) by transferring seven species from the genus *Pseodomonas* homology group II to the new genus. Cells of *Burkholderia* strains were Gram negative, aerobic, straight rods with a single polar flagellum or a tuft of polar flagella when motile. Catalase was usually positive. Genomic DNA GC content was from 59.0 mol% to 69.5 mol%. The genus' specific feature, primarily differentiating it from *Ralstania*, was the fatty acid 16:0 3-OH (Gillis et al. 1995). By the time of writing, the genus *Burkholderia* contained 71 valid published species. Members of the genus were often found in contaminated soils and waters as well as natural soils, waters, and the rhizosphere of plants (Andreolli et al. 2011; Zhang et al. 2000; Zolg & Ottow 1975; Yoo et al. 2007; Partida-Martinez et al. 2007).

They often degraded low-molecular weight organic compound as well as fixed nitrogen (N_2) (Lu, et al. 2012; Zhang et al. 2000).

2. Materials and methods

Strain A4 was isolated from the arsenite rich soil from Florida by spreading the supernatant of the soil suspension over Difco nutrient agar plate containing 500 ppm As(III). Gram staining was conducted following the description in Skerman (1967). Catalase was tested using 3% peroxide. Oxidase was detected with 1% tetramethyl *p*-phenylenediamine dihydrochloride (Lányi, B. (1987)). To observe the cell morphology, both SEM and TEM samples were prepared. SEM sample preparations followed Bogan et al. (2003). TEM sample preparations were as follows: cells taken from agar plate were fixed using 2.5% glutaraldehyde in a 0.1 M phosphate buffer with a pH 6.8, stained with 2% uranyl acetate on a formvar coated grid, and imaged with transmission microscope (TEM) directly.

Fatty acids analysis was conducted by growing the cells on trypticase soy agar for 48 hours, then 50 mg of biomass was taken for saponification, methylation, and extraction. The product was analyzed by gas chromatography (GC) at the MIDI Company.

Total lipids were extracted from 100 mg freeze dried cells by chloroform/methanol (3:1) twice. The extractants were combined and air dried. The acetone-dissolved part of the extracted lipids was developed with benzene as the solvent on a TLC plate. An iodine vapor-detected spot on the plate with a Rf value of 0.48 was scratched, dialyzed, and identified as unbiquinone-8 by ESI MS at the University of Alabama. The remaining polar lipids were dissolved in 50 μL of chloroform/methanol (1:1) and developed by two-dimensional TLC.

DNA was extracted following the method in Chapter 3 2.3. One μL of the DNA (30-60 ng/μL) was used in PCR amplification using primers: 8F:5'-AGAGTTTGATCMTGGCTCAG-3' and 1525R:5'-AAGGAGGTGWTCCARCC-3'. The cleaned PCR products were sent to the Operon Company for sequencing. The obtained DNA sequences were aligned and edited using BioEdit (Hall, 1999). Utilization of carbon substrate was tested using the Biolog GN2 MicroPlate according to the manufacturer's instruction.

The filter hybridization technique was used to determine DNA-DNA relatedness using DIG-High Prime DNA labeling and detection starter kit II (Roche Applied Science). Dot-Blot hybridization was conducted at 54ºC. Experiments followed the manufacturer's instructions. The dot chemiluminecences were recorded by Kodak electron image film (S03-163), and the dot blackness was quantified by Image J software. Self-hybridization was counted as 100%. Hetero-hybridization was calculated as a percentage of the self-hybridization dot. The mean of the triplicate dots was calculated as the final result of DNA-DNA relatedness. G+C content of strain A4 was analyzed by HPLC at DSMZ following the method described in Mesbah et al. (1989).

3. Results and discussions

The colonies of strain A4 appeared pale yellow, shiny, and with complete margin. The cells were aerobic, Gram stained negative, non-spore-forming, non-motile ovoids or short rods, measuring 0.3-0.6×0.5-3.5 μm (Figure 4-1). Catalase and oxidase were positive.

The results were summarized in Table 4-1. The data in the table showed strain A4 had fatty acid composition similar with that of other *Burkholderia* species and also had the

characteristic 16:0 3OH (Viallard et al. 1998), which was differential from that of *Ralstania*. The major polar lipids included PE, PG, and two amino lipids (see supplemental material S1).

An almost complete partial 16S rDNA sequence of 1441 base pairs (supplementary material S2) was obtained for strain A4. Its closest relatives were *Burkholderia zhejiangensis* CCTCC AB 2010354^T, *Burkholderia glathei* DSM 50014^T, and *Burkholderia sodidicola* KCTC 12081^T with similarities of 99.1%, 97.3% and 96.7%, respectively. Its 16S rDNA similarities with all other type strains in the genus *Burkholdeira* and other relevant genera were all below 96.5%. A selection of the close relatives of strain A4 was used in the construction of a phylogenetic tree. *Burkhoderia metallica* CCUG 54567^T was selected as the outgroup. MrBayes 3.1.2 software was used to calculate the tree (Figure 4-2). The tree was consistent with other trees calculated from Paup*4.0b10 (PPC) maximum parsimony or maximum likely (see supplementary material S2). Both trees showed strain A4 was affiliated to genus *Burkholderia*.

The differential features between strain A4 and closely relevant strains were summarized in Table 4-2. As shown by the data in the table, strain A4 differed from *B. zhejiangensis* CCTCC AB 2010354^T by 28 features, *B. glathei* DSM 50014^T by 14 features, and from *B sordidicola* KCTC 12081^T by 20 features.

Strain A4 had 16S rDNA sequence similarities of 99.1% and 97.3% with the type strains *B. zhejiangensis* CCTCC AB 2010354^T and *B. glathei* DSM 50014^T, respectively. DNA-DNA hybridization was required to confirm its separate species status.

DNA relatedness between strain A4 and *B. glathei* DSM 50014^T (with A4 DNA as the probe) was 49 %. Reciprocal relatedness (with *B. glathei* DSM 50014^T DNA as the probe) was 31%. Considering the result error of about 10%, these results were far below the borderline of 70%, hence strain A4 represents a separate species from *B. glathei* DSM 50014^T. The genomic

DNA G+C content of strain A4 was 63.5 mol%. The genomic differences between strain A4 and *B. zhejiangensis* CCTCC AB2010354^T listed in Table 4-3, and compared with other adjacent species pairs in the genus *Burkhoderia*. The data in the Table supported that strain A4 and *B. zhejiangensis* CCTCC AB2010354^T were separate genomic species.

According to the results above, strain A4 is affiliated to the genus *Burkholderia* and can be easily differentiated from its close type strains in the genus. Hence, strain A4 represents a novel species in the genus *Burkholderia*, for which the name *Burkholderia arsenicoxidans* sp. nov. is proposed.

Description of *Burkholderia arsenicoxydans* sp. nov. *Burkholderia arsenicoxidans* (*ar.se.nic.ox'y.dans*. L. n. *arsenicum*, arsenic; N. L. v. *oxydare*, to oxidize; N. L. part. adj. *arsenicoxydans*, arsenic-oxidizing).

Cells are aerobic, Gram negative, non-spore-forming, non-motile short rods or ovoids, measuring 0.3-0.6×0.5-3.5 μm. Catalase and oxidase are positive. Colonies appear as pale yellow color, shiny with complete margin. Its major fatty acids include $C_{18:1}$ ω7c (37.8%), $C_{16:0}$ (20.0%), Summed feature 3 (10.3%), $C_{17:0}$ cyclo (9.6%), $C_{19:0}$ ω8c (5.5%), $C_{16:0}$ 3OH (3.6%), $C_{16:0}$ 2OH (2.9%). Its polar lipids include PE, PG, and an unidentified phospholipid and one aminolipid. Major respiratory quinone is ubiquinone-8. Utilize dextrin, tween 40, tween 80, N-acetyl-D-glucosamine, L-arabinose, D-arabitol, D-fructose, L-fucose, D-galactose, α-D-glucose, m-inositol, lactulose, maltose, D-manitol, D-mannose, D-piscose, L-rhamnose, D-sorbitol, D-trehalose, xylitol, pyruvic acid methyl ester, succinic acid-mono-methyl ester, acetic acid, cis-aconitic acid, citric acid, formic acid, D-galactonic acid lactone, D-galacturonic acid, D-gluconic acid, D-glucosaminic acid, D-glucuronic acid, β-hydroxybutyric acid, p-hydroxyphenlyacetic acid, α-ketoglutaric acid, D, L-lactic acid, propionic acid, quinic acid, D-saccharic acid, sebacic

acid, succinic acid, bromosuccinic acid, succinamic acid, glucuronamide, L-alaninamide, L-alanine, L-alanyl-glycine, L-asparagine, L-aspartic acid, L-glutamic acid, glycyl-L-aspartic acid, glycyl-L-glutamic acid, L-histidine, hydroxy-L-proline, L-leucine, L-ornithine, L-phenylalanine, L-proline, L-pyroglutamic acid, L-serine, L-threonine, D, L-carnitine, γ-aminobutyric acid, urocanic acid, α-D-glucose-1-phosphate, D-glucose-6-phospate. Not utilize α-cyclodextrin, glycogen, N-acetyl-D-galactosamine, adonitol, i-erythritol, D-cellobiose, gentiobiose, α-D-lactose, D-melibiose, β-methyl-D-glucoside, D-raffinose, sucrose, turanose, α-hydroxybutyric acid, γ-hydroxybutyric acid, itaconic acid, α-ketobutyric acid, α-ketovaleric acid, malonic acid, D-alanine, D-serine, inosine, uridine, thymidine, phenylethyl-amine, putrescine, 2-aminoethanol, 2, 3-butanediol, glycerol, D, L, α-glycerol-phosphate. Its genomic DNA G+C content is 63.5 mol%.

The type strain, A4^{T} (= ATCC BAA-2404^{T} =CCTCC AB 2012027^{T}), was isolated from an arsenic trioxide spiked soil in Florida, USA.

References

Andreolli, M., Lampis, S., Zenaro, E., Salkinoja-Salonen, M., Vallini, G. 2011. *Burkholderia fungorum* DBT1: a promising bacterial strain for bioremediation of PAHs-contaminated soils. Fems Microbiology Letters. 319: 11-18.

Bogan, B. W., Sullivan, W. R., Kayser1, K. J., Derr1, KD., Aldrich, H. C., Paterek, J. R. 2003. Alkanindiges illinoisensis gen. nov., sp. nov., an obligately hydrocarbonoclastic, aerobic squalane-degrading bacterium isolated from oilfield soils. International Journal of Systematic and Evolutionary Microbiology. 53(5): 1389-1395.

Coenye, T., Laevens, S., Willems, A., Ohlen, M., Hannant, W., Govan, J. R. W., Gillis, M., Falsen, E., Vandamme, P. 2001. *Burkholderia fungorum* sp. nov., and *Burkholderia caledonica* sp. nov., two new species isolated from the environment, animals and human clinical samples. International Journal of Systematic and Evolutionary Microbiology. 51: 1099-1107.

Gillis, M., Vanvan, T., Bardin, R., Goor, M., Hebbar, P., Willems, A., Segers, P., Segers, K., Heulin, T., Fernandez, M. P. 1995. Polyphasic taxonomy in the genus *Burkholderia* leading to an emended description of the genus and proposition of *Burkholderia vietnamiensis* sp. nov. for N_2-fixing isolates from rice in Vietnam. International Journal of Systematic Bacteriology. 45(2): 274-289.

Hall, T. A. 1999. BioEdit: A user friendly biological sequence alignment editor and analysis program for Windows 95/98/NT. Nucleic Acids Symposium Series. 41: 95-98.

Lányi, B. 1987. Classical and rapid identification methods for medically important bacteria. Methods in Microbiology. 19: 1–67.

Lim, Y. W., Baik, K. S., Han, S. K., Kim, S. B., Bae, K. S. 2003. *Burkholderia sordidicola* sp. nov., isolated from the white-rot fungus *Phanerochaete sordida*. International Journal of Systematic and Evolutionary Microbiology. 53: 1631-1636.

Lu, P., Zheng, L. Q., Sun, J. J., Liu, H. M., Li, S. P., Hong, Q., Li, W. J. 2012. *Burkholderia zhejiangensis* sp. nov., a methyl-parathion-degrading bacterium isolated from a wastewater-treatment system. International Journal of Systematic and Evolutionary Microbiology. 62:1337-1341.

Mesba, M., Premachandran, U., Whitman, W. 1989. Precise measurement of the G+C content of deoxyribonucleic acid by high performance liquid chromatography. International Journal of Systematic Bacteriology. 39: 159-167.

Partida-Martinez, L. P., Groth, I., Schmitt, I., Richter, W., Roth, M., Hertweck, C. 2007. *Burkholderia rhizoxinica* sp. nov. and *Burkholderia endofungorum* sp. nov., bacterial endosymbionts of the plant-pathogenic fungus *Rhizopus microsporus*. International Journal of Systematic and Evolutionary Microbiology. 57: 2583-2590.

Skerman, V. B. D. (1967). A guide to the identification of the genera of bacteria, 2nd edn. Baltimore: Williams & Wilkins.

Viallard, V., Poirier, I., Cournoyer, B., Haurat, J., Wiebkin, S., Ophel-Keller, K. & Balandreau, J. 1998. *Burkholderia graminis* sp. nov., a rhizospheric *Burkholderia* species, and reassessment of *Pseudomonas phenazinium*, *Pseudomonas pyrrocinia* and *Pseudomonas glathei* as *Burkholderia*. International Journal of Systematic Bacteriology. 48: 549-563.

Yoo, S. H., Kim, B. Y., Weon, H. Y., Kwon, S. W., Go, S. J., Stackebrand, E. 2007. *Burkholderia soli* sp. nov., isolated from soil cultivated with Korean ginseng. International Journal of Systematic and Evolutionary Microbiology. 57: 122-125.

Yabuuchi, E., Kosako, Y., Oyaizu, H., Yano, I., Hotta, H., Hashimoto, Y., Ezaki, T., Arakawa, M. 1992. Proposal of *Burkholderia* gen. nov. and transfer of seven species of the genus *Pseudomonas* homology group II to the new genus, with the type species *Burkholderia cepacia* (Palleroni and Holmes, 1981) comb. nov. Microbiology and Immunology. 36: 1251-1275.

Zhang, H., Hanada, S., Shigematsu, T., Shibuya, K., Kamagata, Y., Kanagawa, T., Kurane, R. 2000. *Burkholderia kururiensis* sp. nov., a trichloroethylene (TCE)-degrading bacterium isolated from an aquifer polluted with TCE. International Journal of Systematic and Evolutionary Microbiology. 50: 743-749.

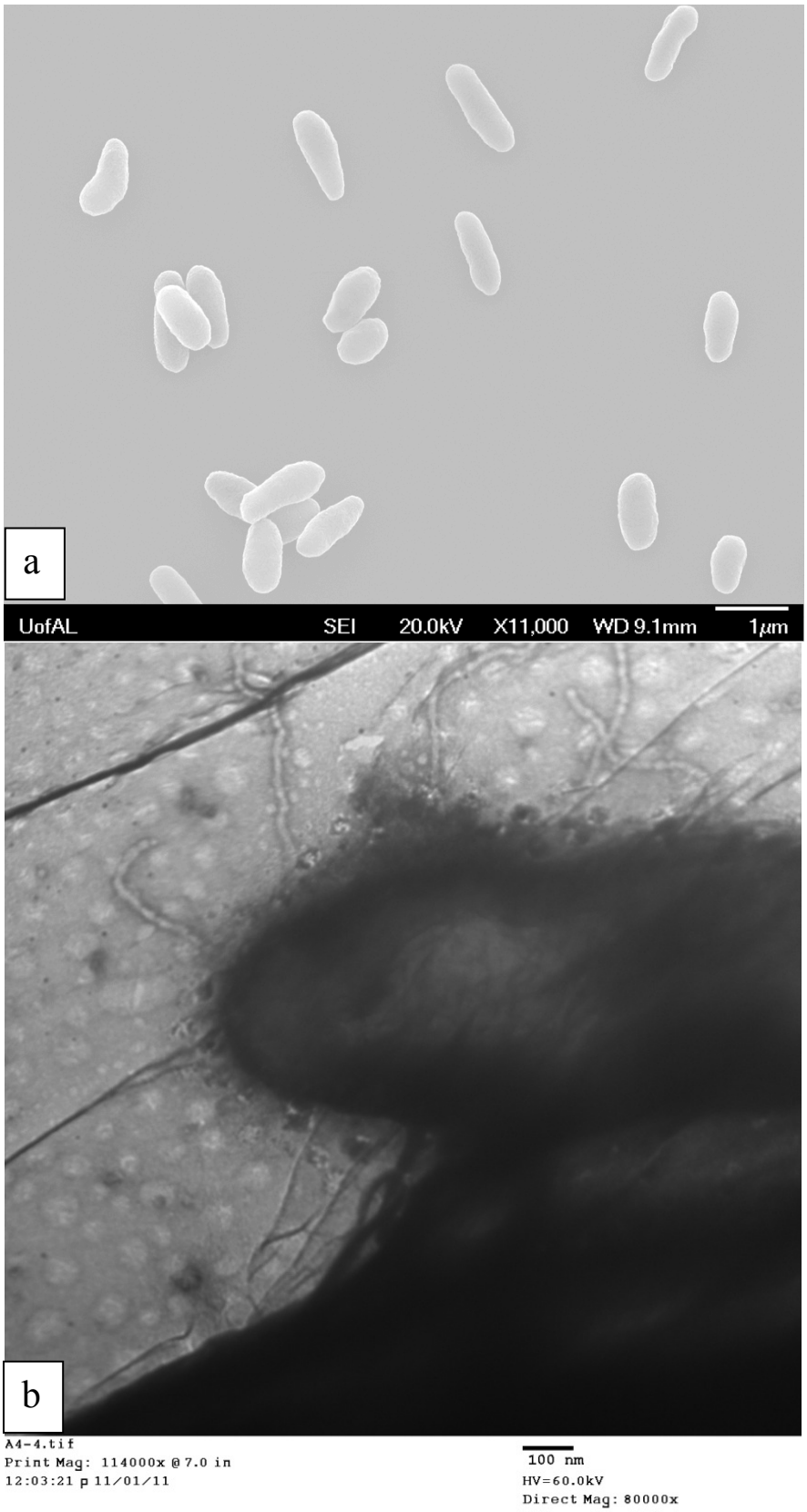

Figure 4-1 SEM(a) and TEM(b) image of strain A4

Table 4-1. Fatty acid composition of relevant strains. 1. Strain A4; 2. *B. zhejiangensis* CCTCC AB2010354^T; 3. *B. glathei* DSM 50014^T, 4. *B. sordidicola* KCTC 12081^T.

Fatty acid	1	2	3	4
10.957	0.23		0.27	-
$C_{12:0}$	-		0.59	0.57
$C_{14:0}$	3.57	5.49	3.81	0.7
Summed feature 2	4.89		5.33	5.06
Summed feature 3	17.41	7.20	17.62	12.45
$C_{16:0}$	18.00	23.38	19.32	18.30
$C_{17:0}$ cyclo	2.23	21.61	7.85	11.00
$C_{16:1}$ 2OH	0.34	1.03	0.19	2.36
$C_{16:0}$ 2OH	1.52	5.66	0.72	2.28
$C_{16:0}$ 3OH	4.14	4.73	4.53	5.06
Summed Feature 5	-			0.36
0.63				
$C_{18:1}$ ω7c	45.00	16.59	36.27	30.80
$C_{18:0}$	0.9		0.74	0.64
$C_{19:0}$ cyclo ω8c	1.04	5.38	1.54	5.35
C19:0	-		0.18	0.34
C18:1 2OH	0.25		0.27	0.64

Summed feature 2 comprises 12:0 aldehyde(?) and/or unknown (ECL= 10.9525)
Summed feature 3 comprises 16:1 ω7c and/or 16:1 w6c.
Summed Feature 5 comprises 18:0 ante and/or 18:2 w6, 9c.

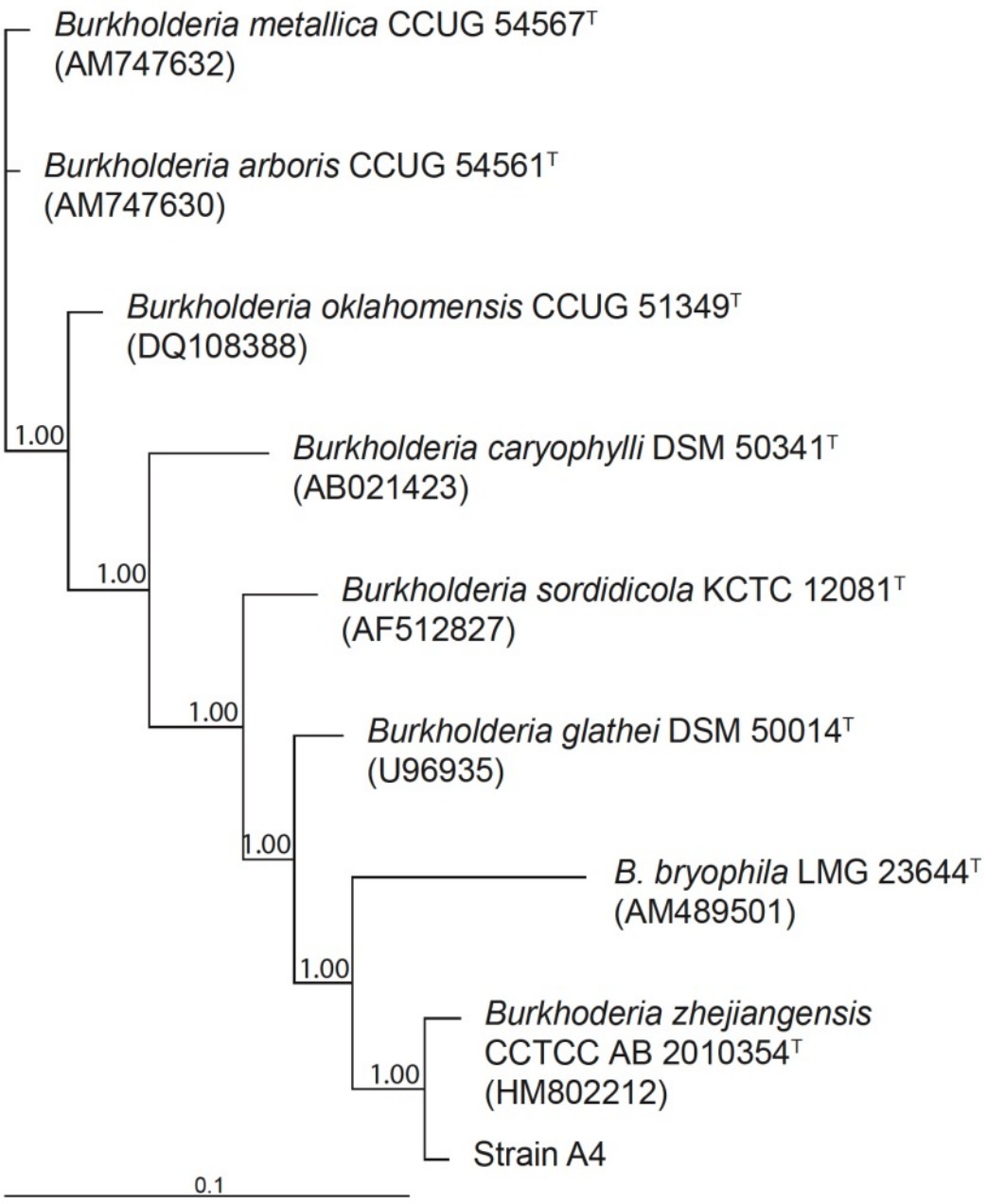

Figure 4-2. The tree was calculated by MrBayes 3.1.2 using GTR model. 600000 generations were run, 6000 trees were sampled, where burnin=2000. The number on the nodes are postscript probability, the bar represented the nucleoside substitution rate per site.

Table 4-2. Differential characteristics of strain A4 and relevant strains.
Strains: 1. Strain A4; 2. *Burkhoderia zhejiangensis* CCTCC AB 2010354^T; 3. *Burkhoderia glathei* DSM 50014^T; 4. *Burkhoderia sordidicola* KCTC 12081^T. +. positive; -, negative; v, variable.

Characteristic	1	2*	3	4
Cell size (μm)	0.3-0.6×1.0-2.8	0.2-0.5×1.0-1.6	0.3-0.7×0.8-2.7	0.5-0.8×1.2-1.8
Cell shape	ovoid to short rod	short rod	short rod	ovoid to short rod
Motility	nonmotile	nonmotile	motile	nonmotile
Flagella	none	none	polar, single	none
Oxidase	+	-	+	+
Nitrate reduction	+	-	+	+
Arsenite oxidation	+	?	+	-
G+C content (mol%)	63.5	59.4	64.8	61.3
Oxidation of				
Glycogen	-	-	+	-
D-Arabitol	+	-	+	+
i-Erythritol	-	-	+	
D-Fructose	+	-	+	+
L-Fucose	+	-	+	+
D-Galactose	+	-	+	+
Lactulose	+	-	+	+
Maltose	+	-	-	-
D-Mannitol	+	-	+	+
Sucrose	-	+	-	-
D-Trehalose	+	-	-	-
Turanose	-	+	-	-
Xylitol	+	-	+	+
Monomethyl succinate	+	-	+	v
Formic acid	+	-	+	v
D-Galactonic acid lactone	+	-	+	v
D-Galacturonic acid	+	+	+	-
D-Gluconic acid	+	-	+	+
D-Glucosaminic acid	+	-	+	+
D-Glucuronic acid	+	-	+	v
γ-Hydroxybutyric Acid	-	-	+	-
p-Hydroxyphenylacetic acid	+	-	+	-
Propionic acid	+	+	+	-
Quinic acid	+	+	+	-
SebacicAcid	+	+	-	-
D-Alanine	+	+	+	-
L-Hydroxyproline	+	-	+	-
L-Leucine	+	+	+	-
L-Ornithine	+	-	-	-
D-Serine	-	+	+	-
D, L-Carnitine	+	+	-	v

Phenylethyl-amine	-	-	+	v
Putrescine	-	+	-	-
2-Aminoethanol	-	+	+	-
2, 3-Butanediol	-		+	
D, L, α-Glycerol-Phosphate	+	-	-	-
α-D-Glucose-1-phosphate	+	-	+	-
D-Glucose-6-phosphate	+	-	+	-

* Data came from Lu et al. 2012, other data came from this study except DNA G+C contents for strains 3 and 4.

Table 4-3 Comparison between genomic features of strain A4 vs. *B. zhejiangensis* CCTCC AB2010354^T and other adjacent species pairs in the genus *Burkhoderia*.

	16S rDNA similarity	G+C content difference
A4 vs. *B. zhejiangensis* CCTCC AB2010354^T	99.1%	63.5 - 59.4=4.1%
B. ubonensis CCUG 48852^T vs. *B. latens* CCUG 54555^T	99.6%	69.71 - 67=2.71%
B. ubonensis CCUG 48852^T vs. *B. vietnamiensis* DSM 11319^T	99.5%	69.71-66.9(68.1)=2.81%

Supplementary Materials

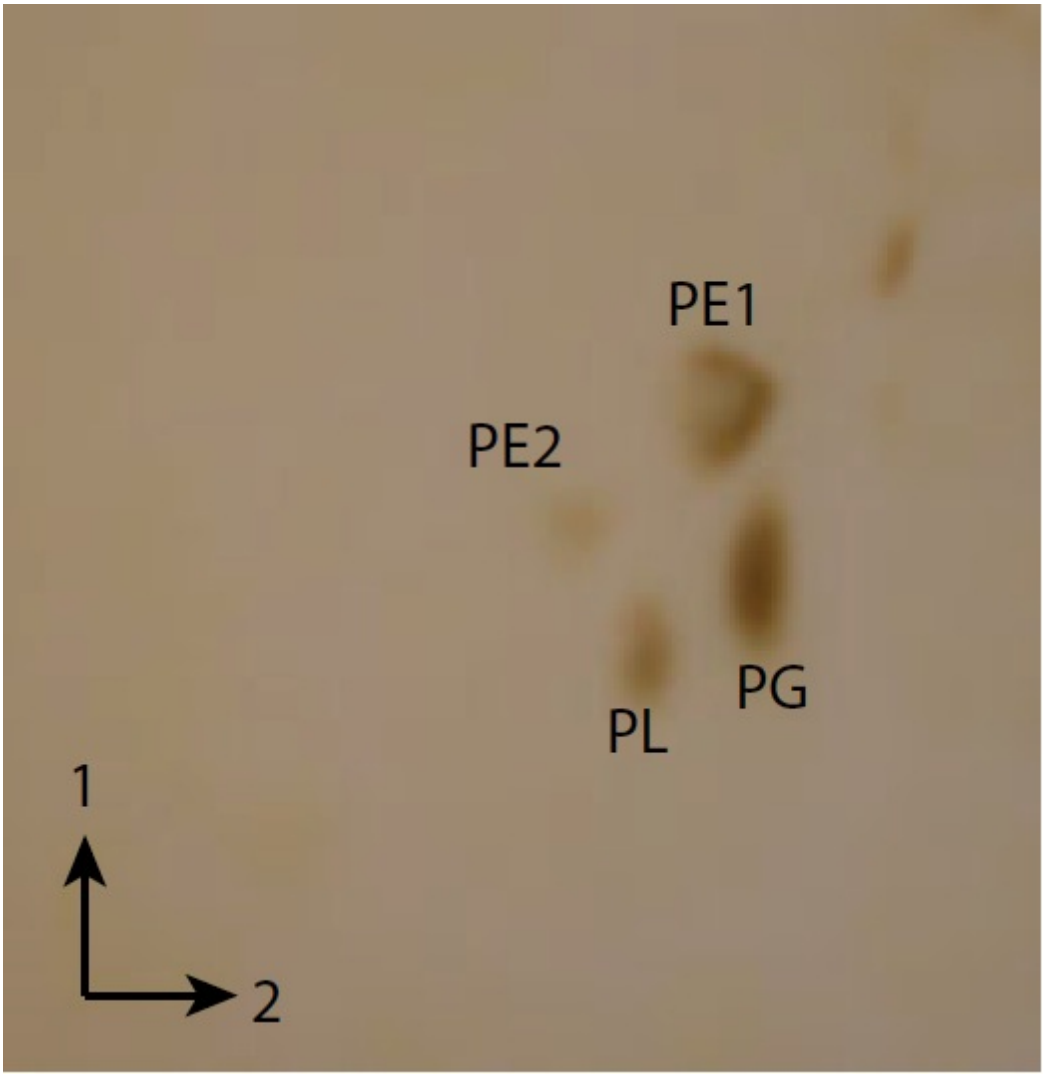

S-1. Polar lipids of strain A4. Stained with molybdophosphoric acid. Solvent for the first diection: chloroform/methanol/water=65/25/4; solvent for the second direction: chloroform/acetic acid/methanol/water=80/18/12/5.

CATGCAAGTCGAACGGCAGCACGGGGGCAACCCTGGTGGCGAGTGGCGAACGGGT
GAGTAATACATCGGAACGTGTCCTGTAGTGGGGGATAGCCCGGCGAAAGCCGGATT
AATACCGCATACGACCTAAGGGAGAAAGCGGGGGATCTTCGGACCTCGCGCTATAG
GGGCGGCCGATGGCAGATTAGCTAGTTGGTGGGGTAAAGGCCTACCAAGGCGACGA
TCTGTAGCTGGTCTGAGAGGACGACCAGCCACACTGGGACTGAGACACGGCCCAGA
CTCCTACGGGAGGCAGCAGTGGGGAATTTTGGACAATGGGGGCAACCCTGATCCAG
CAATGCCGCGTGTGTGAAGAAGGCCTTCGGGTTGTAAAGCACTTTTGTCCGGAAAGA
AAACTTGCGCCCTAATATGGTGCGAGGATGACGGTACCGGAAGAATAAGCACCGGC
TAACTACGTGCCAGCAGCCGCGGTAATACGTAGGGTGCGAGCGTTAATCGGAATTA
CTGGGCGTAAAGCGTGCGCAGGCGGTCTGTTAAGACCGATGTGAAATCCCCGGGCT
TAACCTGGGAACTGCATTGGTGACTGGCAGGCTTTGAGTGTGGCAGAGGGAGGTAG
AATTCCACGTGTAGCAGTGAAATGCGTAGAGATGTGGAGGAATACCGATGGCGAAG
GCAGCCTCCTGGGCCAACACTGACGCTCATGCACGAAAGCGTGGGGAGCAAACAGG
ATTAGATACCCTGGTAGTCCACGCCCTAAACGATGTCAACTAGTTGTTGGGGATTCA
TTTCCTTAGTAACGTAGCTAACGCGTGAAGTTGACCGCCTGGGGAGTACGGTCGCAA
GATTAAAACTCAAAGGAATTGACGGGGACCCGCACAAGCGGTGGATGATGTGGATT
AATTCGATGCAACGCGAAAAACCTTACCTACCCTTGACATGGTCGGAATCCTGCTGA
GAGGCGGGAGTGCTCGAAAGAGAACCGACGCACAGGTGCTGCATGGCTGTCGTCAG
CTCGTGTCGTGAGATGTTGGGTTAAGTCCCGCAACGAGCGCAACCCTTGTCCTTAGT
TGCTACGCAAGAGCACTCTAAGGAGACTGCCGGTGACAAACCGGAGGAAGGTGGGG
ATGACGTCAAGTCCTCATGGCCCTTATGGGTAGGGCTTCACACGTCATACAATGGTC
GGAACAGAGGGTTGCCAAGCCGCGAGGTGGAGCCAATCCCAGAAAACCGATCGTA
GTCCGGATCGCAGTCTGCAACTCGACTGCGTGAAGCTGGAATCGCTAGTAATCGCGG
ATCAGCATGCCGCGGTGAATACGTTCCCGGGTCTTGTACACACCGCCCGTCACACCA
TGGGAGTGGGTTTCACCAGAAGTAGGTAGCCTAACCGCAAGGAGGGCGCTTACCAC
GGTGGGATTCATGACTGGGGTGAAGTCGTAACAAG

S2. 1441 basepairs of 16S rDNA sequence for strain A4.

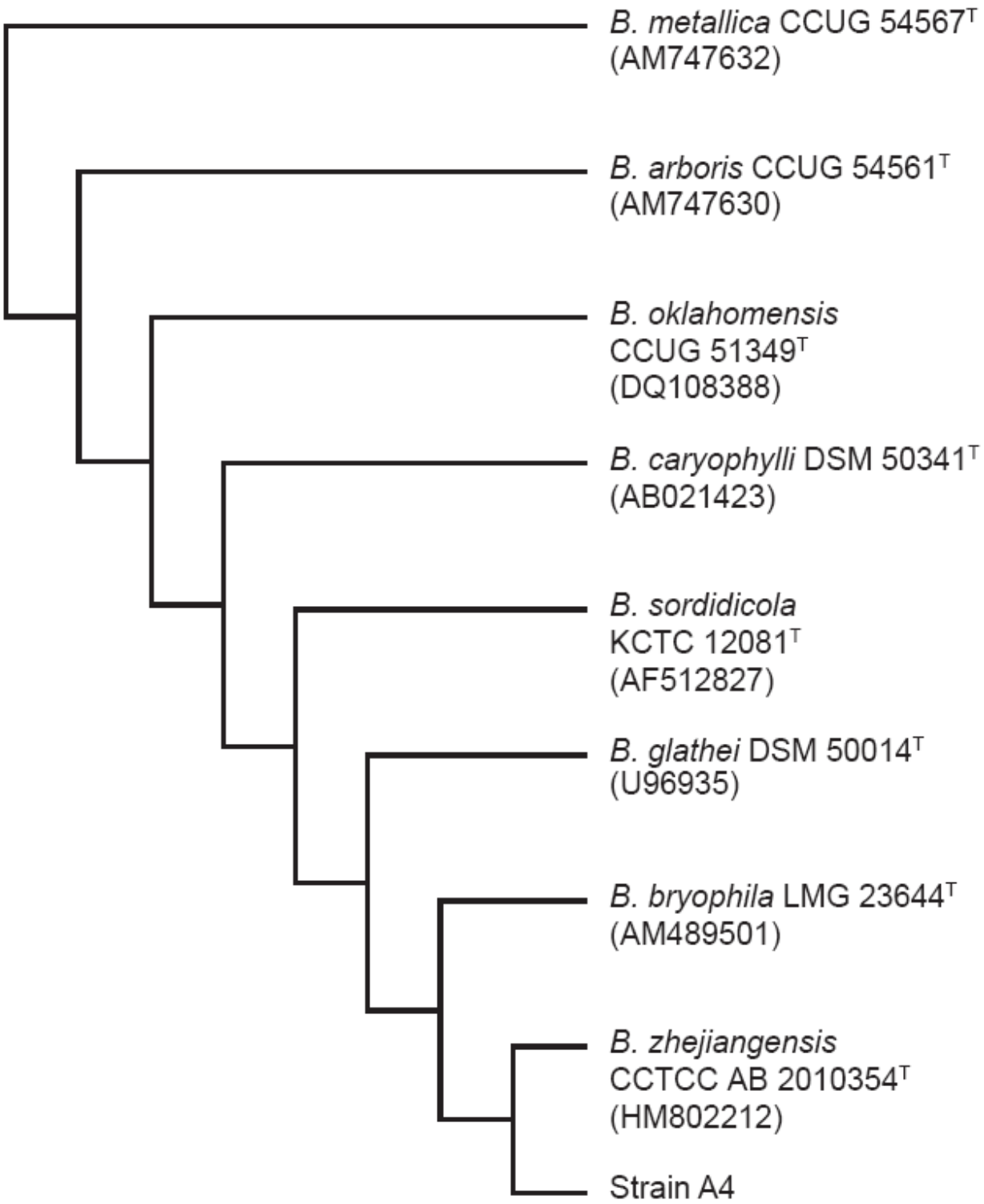

S3. Phylogenetic tree for strain A4 and its close relatives calculated from maximum parsimony method.

CHAPTER 5

SUMMARY

This dissertation started with experimental simulation of arsenic trioxide contamination of soil at an industrial site located in Fort Walton, Florida, which was extended to investigate the As(III) oxidation mechanism, and led to the discovery and characterization of a previously unidentified As(III) oxidizing bacterium. The study resulted in: (1) Experimental simulation of 60 years leaching after arsenic trioxide herbicide application at Fort Walton site, (2) observation that peak arsenic release only lasted the first 200 pore volumes, where As(III) dominated the arsenic speciation, (3) observation that As(V) dominated the arsenic speciation in the arsenic release tail after 200 pore volumes, i.e., rapid As(III) oxidation in the soil column experiments, (4) determination of bacterial As(III) oxidation mechanism in the above experiments, (5) the characterization and nomenclature of an As(III) oxidizing bacterium, *Burkhoderia arsenicoxidans* sp. nov., (6) development of a new method for As(V) analysis using current DIONEX ion chromatograph, (7) development of a new method to test if a bacterial strain can oxidize As(III).

As discussed in Chapter 2 detailing the study of arsenic leachability, mobility, and toxicity in arsenic-spiked soil column experiments, it has been found that leached arsenic converted from As(III) state to As(V) state within the soil column (residence time of approximately 6.5 hours) after 180 pore volumes. Although previous research observed that soil

arsenic was in As(V) state, such abnormally fast arsenic oxidation within 6.5 hours was not expected. This process reduced arsenic toxicity and mobility.

In Chapter 3, it was determined that the observed fast arsenite oxidation was caused by bacteria. Such efficient arsenite oxidizers include strain A12 (100% match of 16S rDNA sequence with *B. fungorum* LMG 16225^T and strain A4 (99.1% and 97.3% match with *B. zhejiangensis* CCTCC AB 2010354^T and *B. glathei* DSM 50014^T respectively). Strain A12 was a more efficient arsenite oxidizer than strain A4 throughout the experiment. The method to test bacterial As(III) oxidation was a brand new development in this study although previous methods were tried first.

In Chapter 4, a polyphasic characterization was conducted on strain A4 to determine its taxonomic position, including phenotypic and biochemical characterizations, 16S rDNA sequence analysis, DNA-DNA hybridization. The data showed that strain A4 represented a novel species in the genus *Burkholderia*, for which the name *Burkholderia arsenicoxydans* sp. nov. is proposed.

The significance of such findings has prominent effects on our understanding of arsenic contamination and conversion in the environment. The arsenite oxidation by Gram negative bacteria was one of the biological protection mechanisms to prevent arsenic poisoning. The findings of this study can potentially also be used in arsenite remediation of contaminated soil and groundwater, where bacteria can oxidize arsenite into arsenate efficiently and reduce arsenic toxicity and bioavailability.